CLS Run Summer 2016 Logbook

August 23-30, 2016

Participants: Tegan Beattie, Richard Jones, Zisis Papandreou,
Brendan Pratt, and Andrei Semenov

Table of Contents

Goals for this run

1. Measure first rocking curves at CLS using virgin 4x4 sample
2. Quantify the instrumental resolution, understand differences from CHESS
3. Optimize new beam setup with respect to resolution and scan times
4. Take rocking curves of the 7x7 framed diamond in the mylar hoop
5. Align diamond mount ring so we can measure diamond offsets
6. Glue diamond to aluminum tab and allow the epoxy to set
7. Take new set of rocking curves with mounted diamond

CLS Beam Permit document

The document below is posted outside the BMIT endstation area, showing the activity that is happening this week on our beamline.

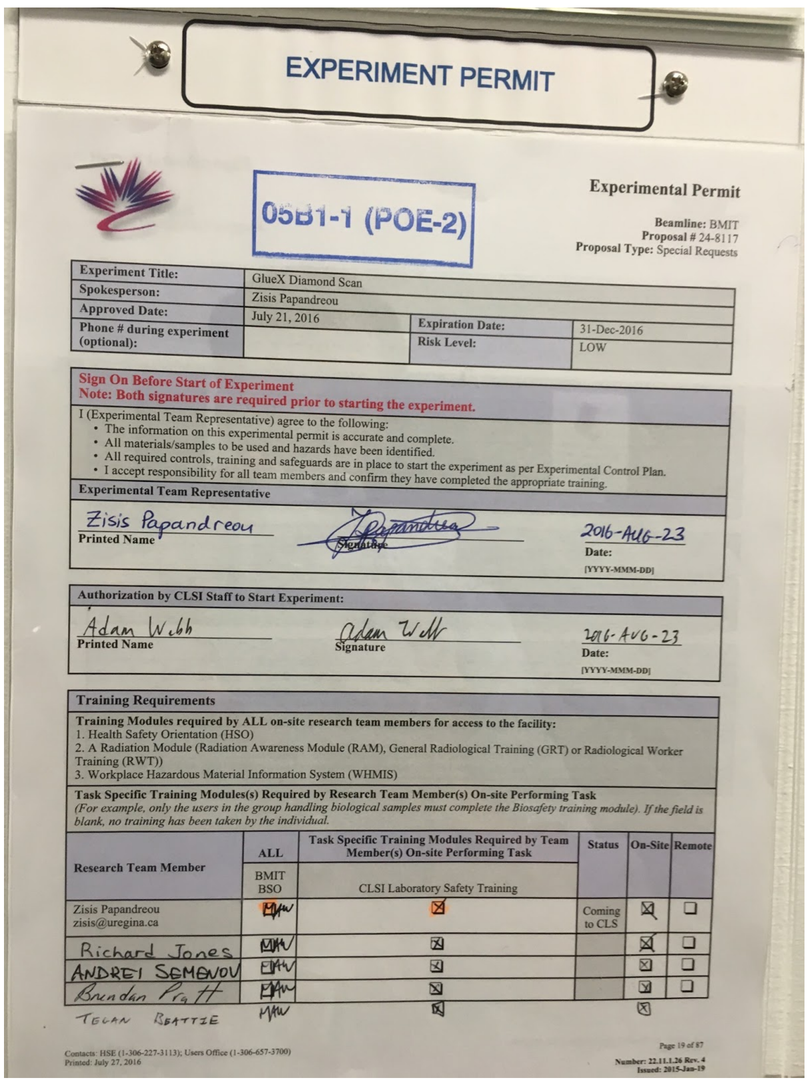

EXPERIMENT PERMIT

05B1-1 (POE-2)

Experimental Permit

Beamline: BMIT
Proposal # 24-8117
Proposal Type: Special Requests

Experiment Title:	GlueX Diamond Scan		
Spokesperson:	Zisis Papandreou		
Approved Date:	July 21, 2016	**Expiration Date:**	31-Dec-2016
Phone # during experiment (optional):		**Risk Level:**	LOW

Sign On Before Start of Experiment
Note: Both signatures are required prior to starting the experiment.

I (Experimental Team Representative) agree to the following:

- The information on this experimental permit is accurate and complete.
- All materials/samples to be used and hazards have been identified.
- All required controls, training and safeguards are in place to start the experiment as per Experimental Control Plan.
- I accept responsibility for all team members and confirm they have completed the appropriate training.

Experimental Team Representative

Zisis Papandreou — Printed Name; [signature] — Signature; 2016-AUG-23 — Date: [YYYY-MMM-DD]

Authorization by CLSI Staff to Start Experiment:

Adam Webb — Printed Name; Adam Webb — Signature; 2016-AUG-23 — Date: [YYYY-MMM-DD]

Training Requirements

Training Modules required by ALL on-site research team members for access to the facility:
1. Health Safety Orientation (HSO)
2. A Radiation Module (Radiation Awareness Module (RAM), General Radiological Training (GRT) or Radiological Worker Training (RWT))
3. Workplace Hazardous Material Information System (WHMIS)

Task Specific Training Modules(s) Required by Research Team Member(s) On-site Performing Task
(For example, only the users in the group handling biological samples must complete the Biosafety training module). If the field is blank, no training has been taken by the individual.

Research Team Member	ALL: BMIT BSO	Task Specific Training Modules Required by Team Member(s) On-site Performing Task: CLSI Laboratory Safety Training	Status	On-Site	Remote
Zisis Papandreou zisis@uregina.ca	☒ MAW	☒	Coming to CLS	☒	☐
Richard Jones	☒ MAW	☒		☒	☐
ANDREI SEMENOV	☒ MAW	☒		☒	☐
Brendan Pratt	☒ MAW	☒		☒	☐
TEGAN BEATTIE	MAW	☒		☒	

Contacts: HSE (1-306-227-3113); Users Office (1-306-657-3700)
Printed: July 27, 2016

Page 19 of 87
Number: 22.11.1.26 Rev. 4
Issued: 2015-Jan-19

Useful Information

- Phone numbers
    a. Zisis Papandreou, email: zisis@uregina.ca, cell: 306-596-7775
    b. Andrei Semenov, email: semenov@jlab.org, cell: 306-502-5291
    c. Tegan Beattie, email: beattite@uregina.ca, cell: 306-737-2541
    d. Brendan Pratt: 860-617-8138
    e. Richard Jones: 860-377-5224
    f. George Belev, BMIT Staff Scientist, office: 306-657-3814, cell: 306-261-2065
    g. Adam Webb, BMIT Science Associate, office: 306-657-3846, cell: 306-372-8304
    h. Nazanin Samadi, BMIT Technical Assistant, cell: 306-717-5469
    i. BMIT and other CLS phone numbers: see image below

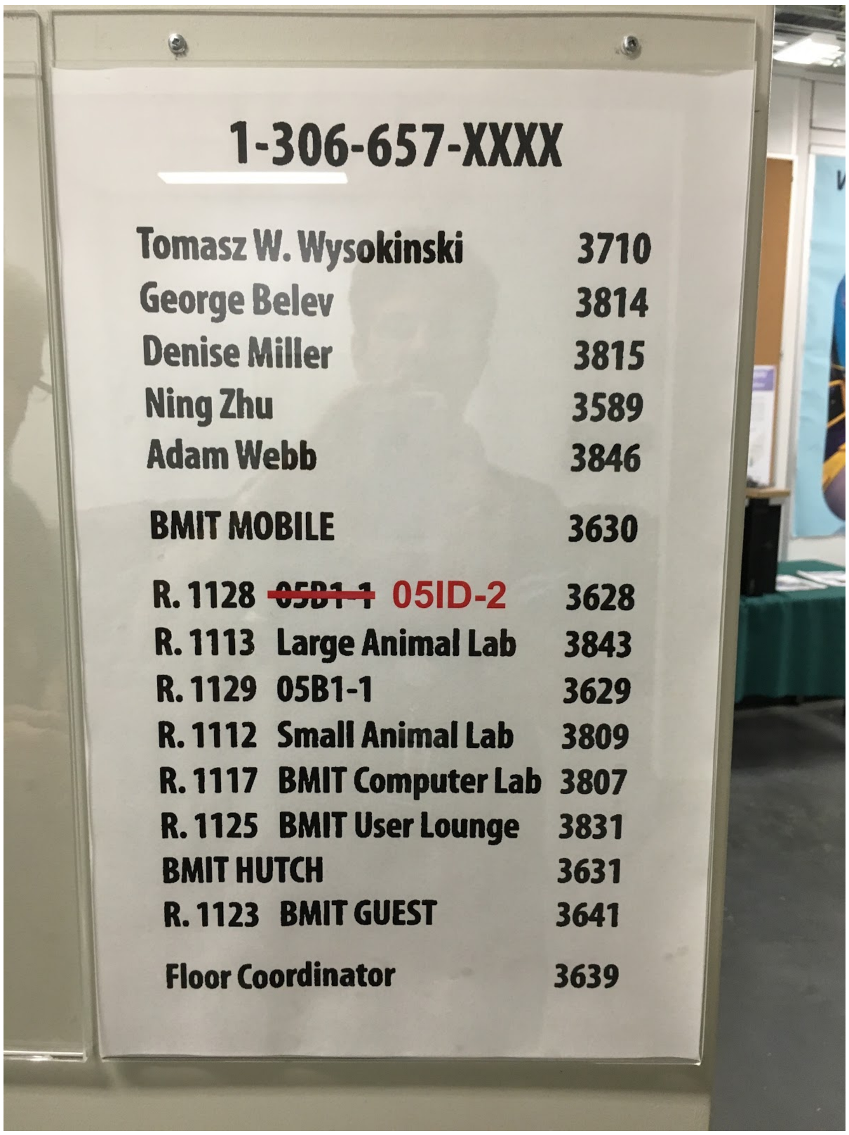

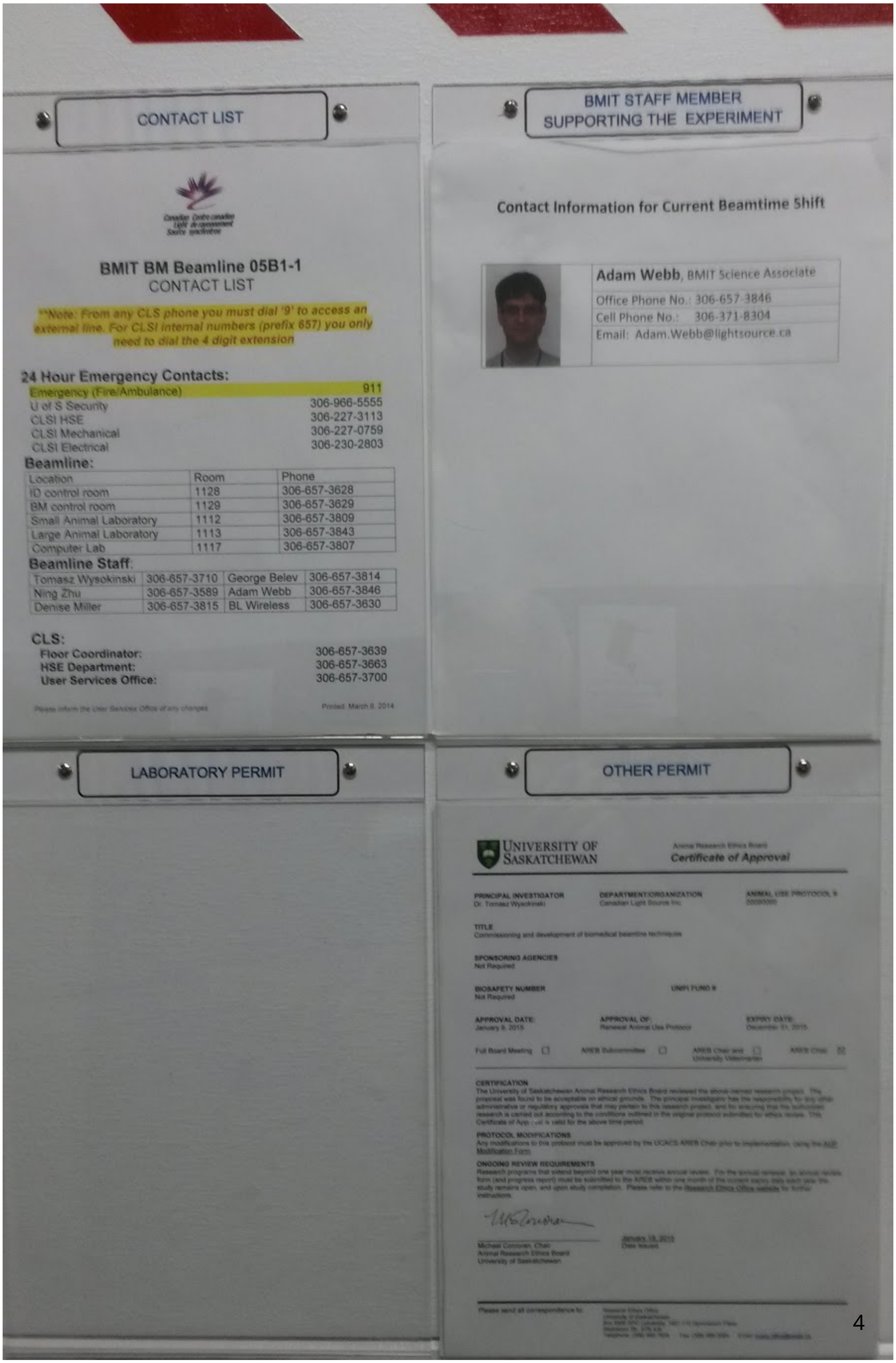
CONTACT LIST
BMIT BM Beamline 05B1-1
CONTACT LIST
**Note: From any CLS phone you must dial '9' to access an external line. For CLSI internal numbers (prefix 657) you only need to dial the 4 digit extension
24 Hour Emergency Contacts:
Emergency (Fire/Ambulance) 911
U of S Security 306-966-5555
CLSI HSE 306-227-3113
CLSI Mechanical 306-227-0759
CLSI Electrical 306-230-2803
Beamline:
Location | Room | Phone
ID control room | 1128 | 306-657-3628
BM control room | 1129 | 306-657-3629
Small Animal Laboratory | 1112 | 306-657-3809
Large Animal Laboratory | 1113 | 306-657-3843
Computer Lab | 1117 | 306-657-3807
Beamline Staff:
Tomasz Wysokinski 306-657-3710 | George Belev 306-657-3814
Ning Zhu 306-657-3589 | Adam Webb 306-657-3846
Denise Miller 306-657-3815 | BL Wireless 306-657-3630
CLS:
Floor Coordinator: 306-657-3639
HSE Department: 306-657-3663
User Services Office: 306-657-3700
BMIT STAFF MEMBER SUPPORTING THE EXPERIMENT
Contact Information for Current Beamtime Shift
Adam Webb, BMIT Science Associate
Office Phone No.: 306-657-3846
Cell Phone No.: 306-371-8304
Email: Adam.Webb@lightsource.ca
LABORATORY PERMIT
OTHER PERMIT
UNIVERSITY OF SASKATCHEWAN
Certificate of Approval
PRINCIPAL INVESTIGATOR
DEPARTMENT/ORGANIZATION
TITLE
SPONSORING AGENCIES
BIOSAFETY NUMBER
APPROVAL DATE:
APPROVAL OF:
EXPIRY DATE:
CERTIFICATION
PROTOCOL MODIFICATIONS
ONGOING REVIEW REQUIREMENTS

- Most of the data acquisition computers run Windows, and most DAQ applications are LabView based. From left to right on the control room desktop we have:
    a. wks-w000772 (local Windows desktop)
    b. bmit-ni-2 (Windows remote desktop, bottom screen, reads mono settings)
    c. opi1128-003 (Linux remote desktop, two top screens, beamline control)
    d. electron4, login PXIe (Windows remote desktop, bottom screen)

- The one exception to this is the machine that runs the EPICS interface, which is a Linux machine called opi1128-003.

- To take a screenshot: from within LabView, press ctrl-P, select Adobe PDF for the printer choice, and do Print. Then select the output folder where the print file should be written and press OK. Then go to the output folder and send the screenshot image file to the desired destination.

- How to print to the BMIT control room printer: the print server for the printers attached to the endstations is vsrv-print-01. The printer name is posted next to the printer. Looking at wks-w000772, we see that the local printer behind the control bench in the control room is prd-ljm451-e-0. If you want to print, you need to go to wks-w000772 and fetch the file, then print from that machine.
- PDF of the stepper motors used for the goniometer (model SA16A-RS)

- Here is a list of all of the GUIs that we need to know about to do scans.

    a. fast shutter - electron4 Labview gui called FAST SHUTTER on the vi panel. In the Labview project file list, this vi is called “Shutter control ver1.vi”.
    b. beam shutters upstream of the fast shutter - opi1128-003 has gui panel called BMIT-BM-Main (EPICS application, not Labview). This opens a graphical view of the beamline with a large green indicator that says BEAM ON when beam is present in POE-2, and disappears when not. The “Beam On” action button opens all shutters in the correct order (order matters!). Normally you don’t have to do “Beam Off” on the gui, as pressing the corresponding button on the ASICS panel does the same thing.
    c. filters on the main beamline - opi1128-003 has a graphical view of the beamline, and on the graphic image are text labels like “Filters”. Click on “Filters” to bring up a special GUI for controlling the filters. If there is beam in POE-1, the filter GUI will not allow you change anything. To close the shutter to POE-1, you need to close Front End Photon Shutter PSH-2. There are 3 filter positions to be switched in or out. Our 20keV configuration is:
        i. filter 1u (aluminum 0.1 mm)
        ii. filter 2m (aluminum 1 mm)

iii. open (none)

d. beam slits in POE-2 hutch - at the top right of the EPICS screen is a button called "Set Beam Dimensions". To modify this, you need to know the distance from the bend magnet to the sample state, which is 25 m. After this you can enter the horizontal and vertical sizes of the beam, and its offset from the nominal beamline axis.
e. monochromator - in the center of the EPICS screen is a button called "Mono". Clicking this button brings up a gui for controlling the monochromator. The most significant entry box is "Energy" at the bottom of the monochromator gui. Once this is updated, the mono angles will automatically update to be consistent with the new setting.
f. piezoFeedback - Labview main program that is used to micro-tweak the mono is called PiezoFeedback-monochromator. If you think the beam intensity is low relative to the stored current in the ring, a fine tweak to the mono might be useful to recover full intensity.
g. Table2_ptch_stage.vi opens up to a window with a big text box "Pitch" in the upper left corner. This controls the pitch degree of freedom of the sample holder. The pitch motor controls the Bragg angle, and is currently connected to motor axis 7 (cable 3 in the hutch). The lead screw pitch is 1.4184 (called "Tall stage" in the GUI hint). The "Travel Distance" field controls the stage step size (degrees). The driver microstep value is 2 (default is right), and the motor steps per rev is 500 (default is correct). The velocity can be adjusted, but its default value is 0.5 deg/s which is fairly fast. Running this gui causes it to execute one step and then halt.
h. Table2_roll_stage.vi opens up to a window with a big text box "Roll" at the top. Here the opposite choice must be made for the lead screw pitch (1.6667, short stage). Right now the motor is not connected to a controller wire, so to use this motor, switch the cable from one of the other motors, and then this gui should work.
i. Table2_rot_stage.vi opens up to a window with a big text box "Rotation (Yaw)" at the top. Here the choice for lead screw pitch is 0.5 rev/deg. This one is wired currently on axis 8 (cable 4, cable number = axis number - 4).
j. Table2_horizontal_stage.vi opens up to a window with a big text box "Horizontal" at the top. This gui is currently borrowed for the use of the vertical displacement of the camera. It is connected to axis 5 (cable 1) currently. The lead screw defaults to 1 rev/mm, which is correct for that motor as well.
k. Table2_vertical_stage.vi opens up to a window with a big text box "Sample Vertical" at the top. This is connected to axis 6 (cable 2) currently. Its lead screw defaults to 1 rev/mm, which is correct.
l. 2D-step&shoot_scan-UofR.vi is the main vi that we will need to use for doing rocking curve scans.

- Link to the work spreadsheet where X-ray optics and target properties data were collected and analyzed.

Setup Photos

Phosphor screen in front of camera/detector to determine diamond scatter position

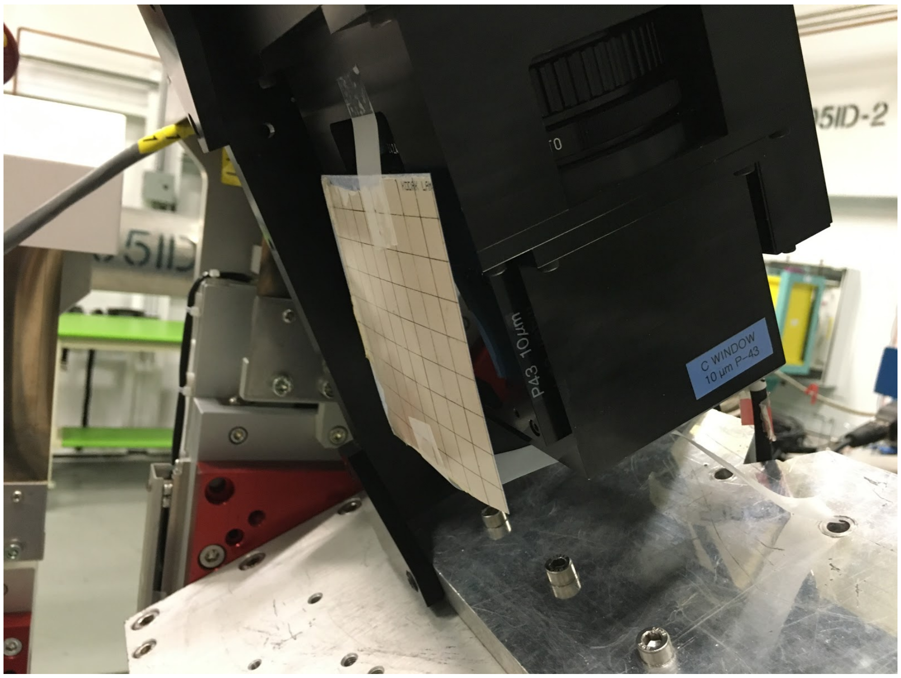

Instructions for rocking curve scans

August 24, 2016 [rtj]

Three gui's running on two different computers must work together in order to take rocking curve scans.

1. EPICS beamline controls gui
2. 2D-step&shoot_scan-UofR.vi running on electron4
3. HCImageLive application running on bmit-ni-2

Here are snapshots of these three applications when they are setup for running a scan.

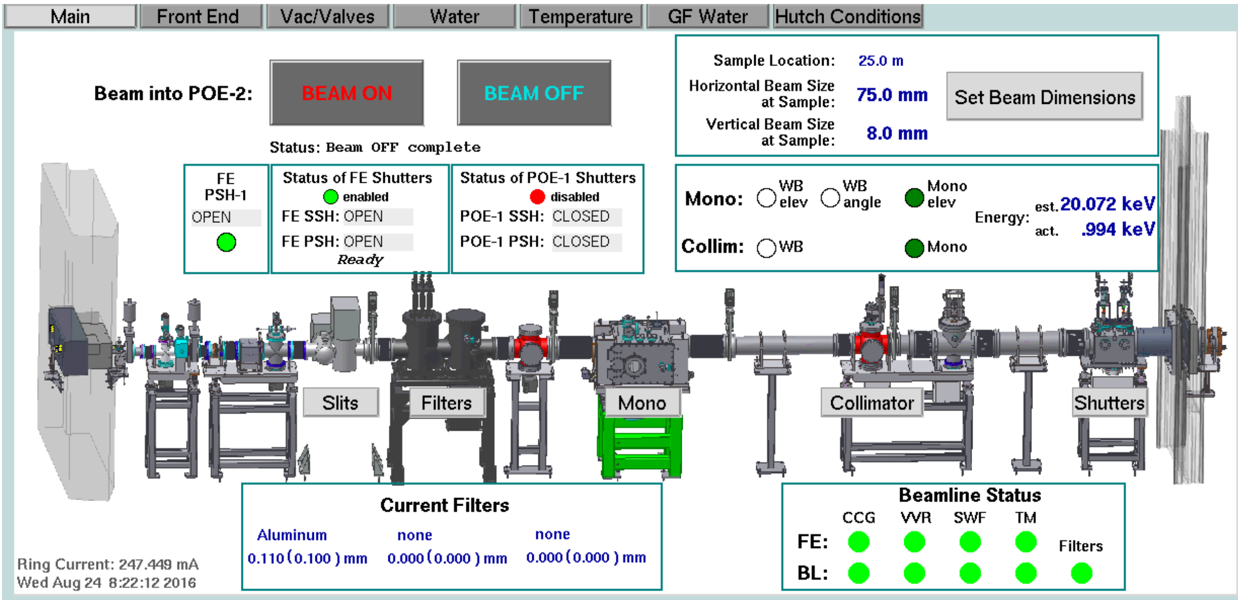

Main beamline controls gui (top left screen)

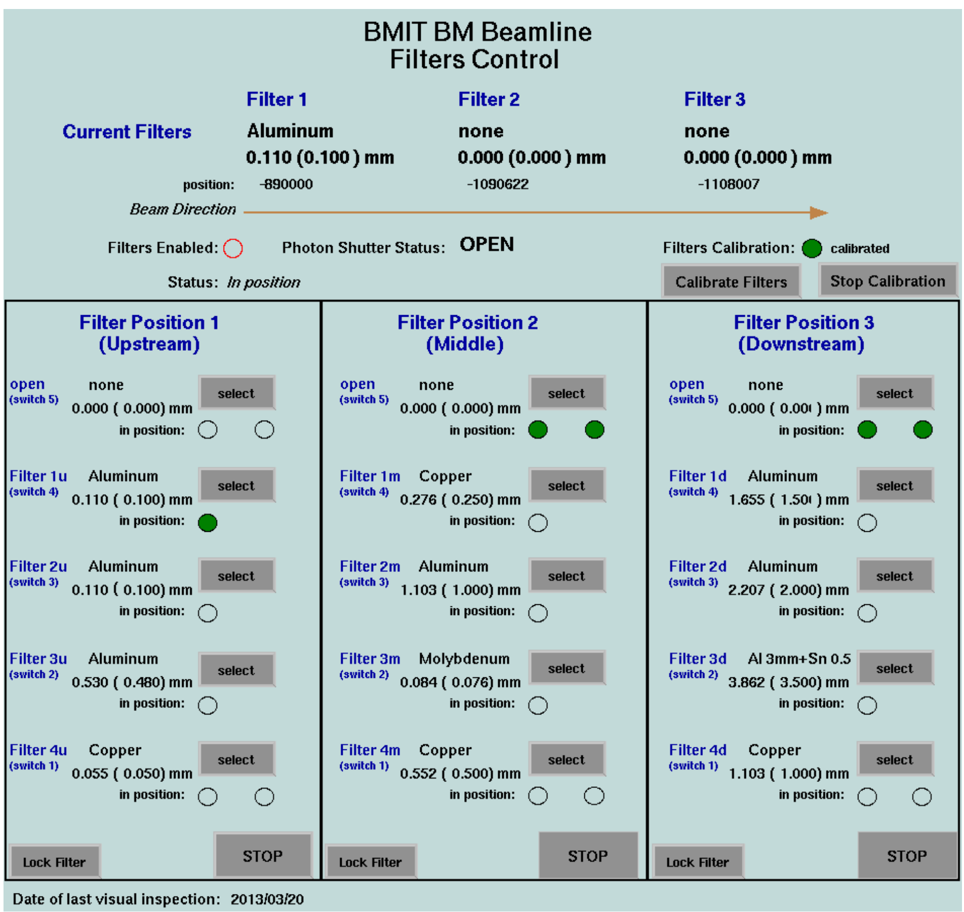

beamline filters control gui (top left screen)

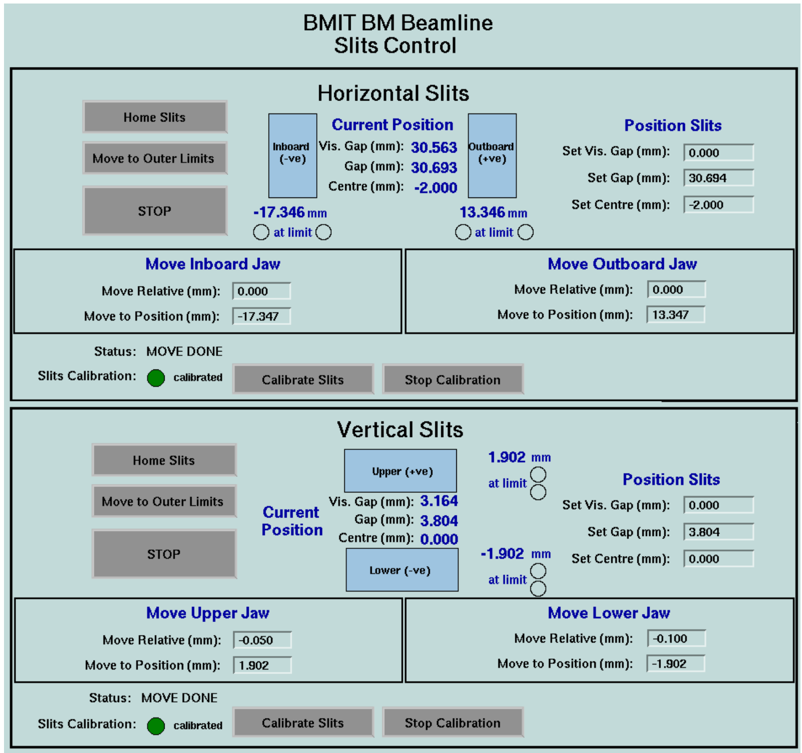

main beamline slits control gui (top left screen)

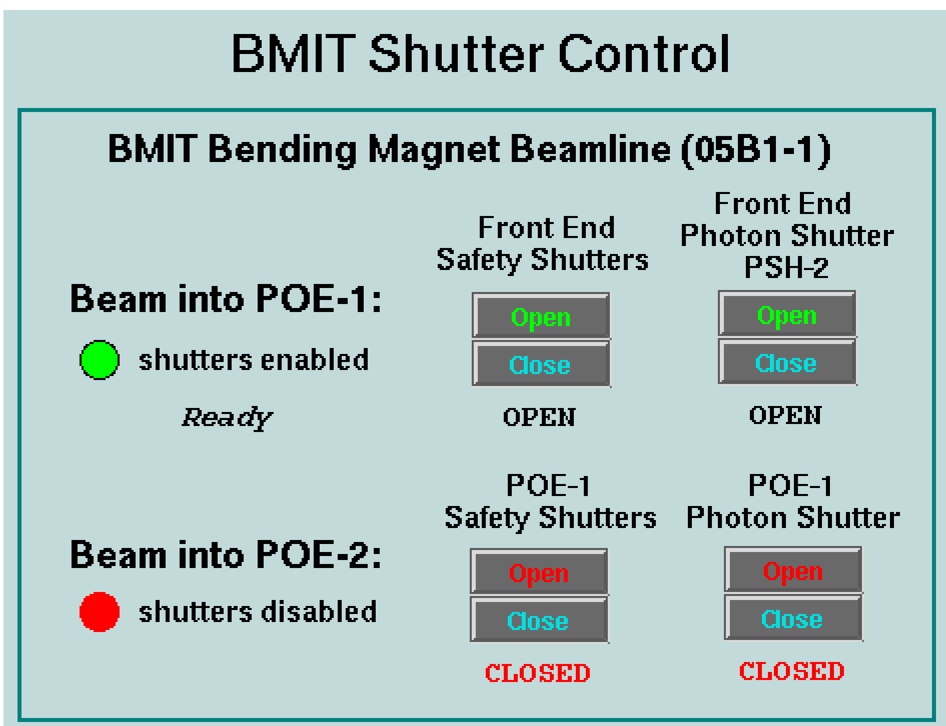

main beamline shutter controls gui (top left screen)

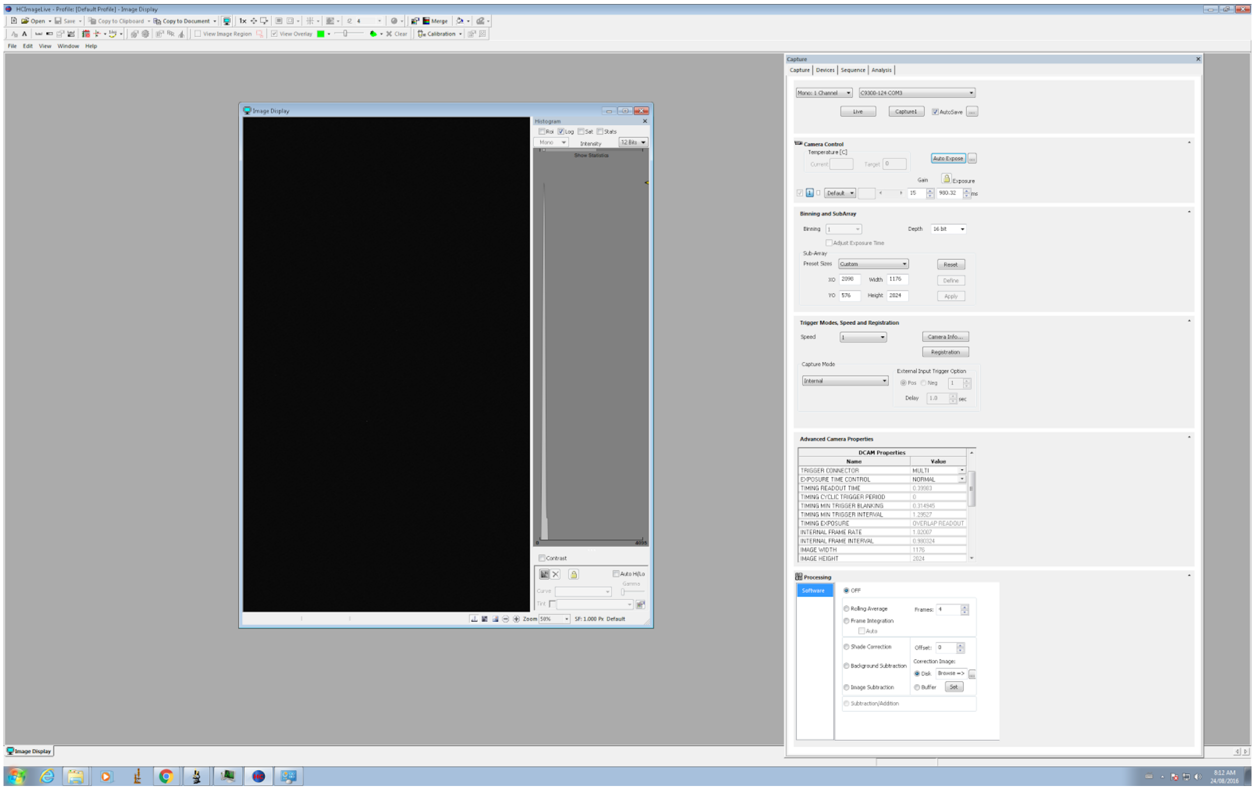

fullscreen gui HCImageLive (camera control gui, lower left screen)

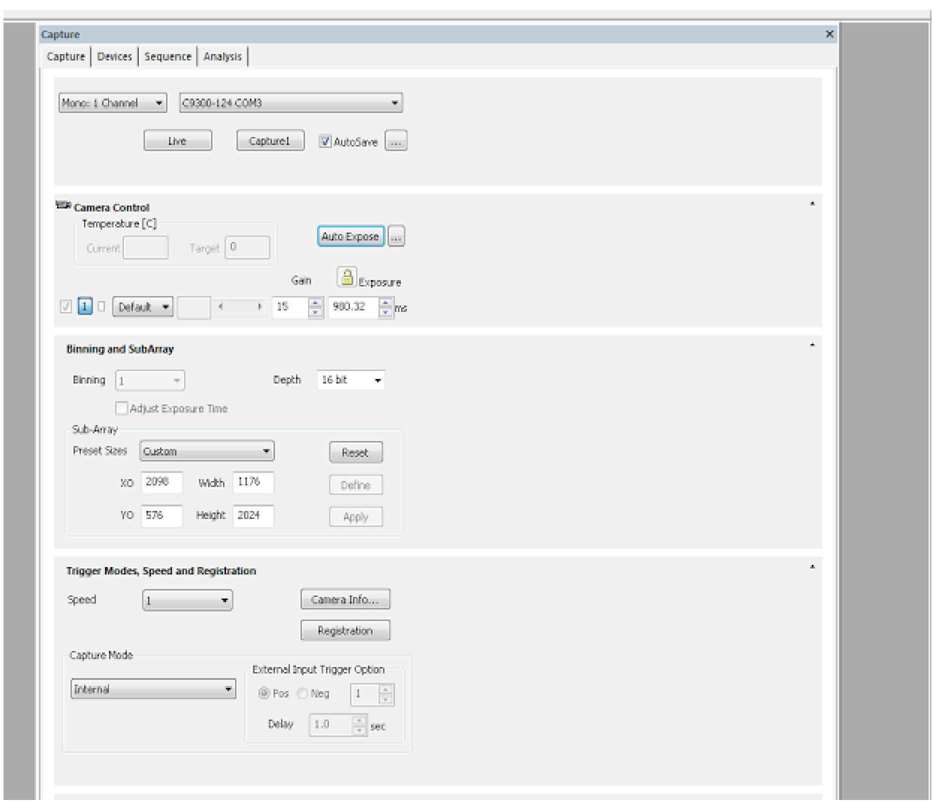

expanded view of the above gui, Capture pane (right-hand side of screen)

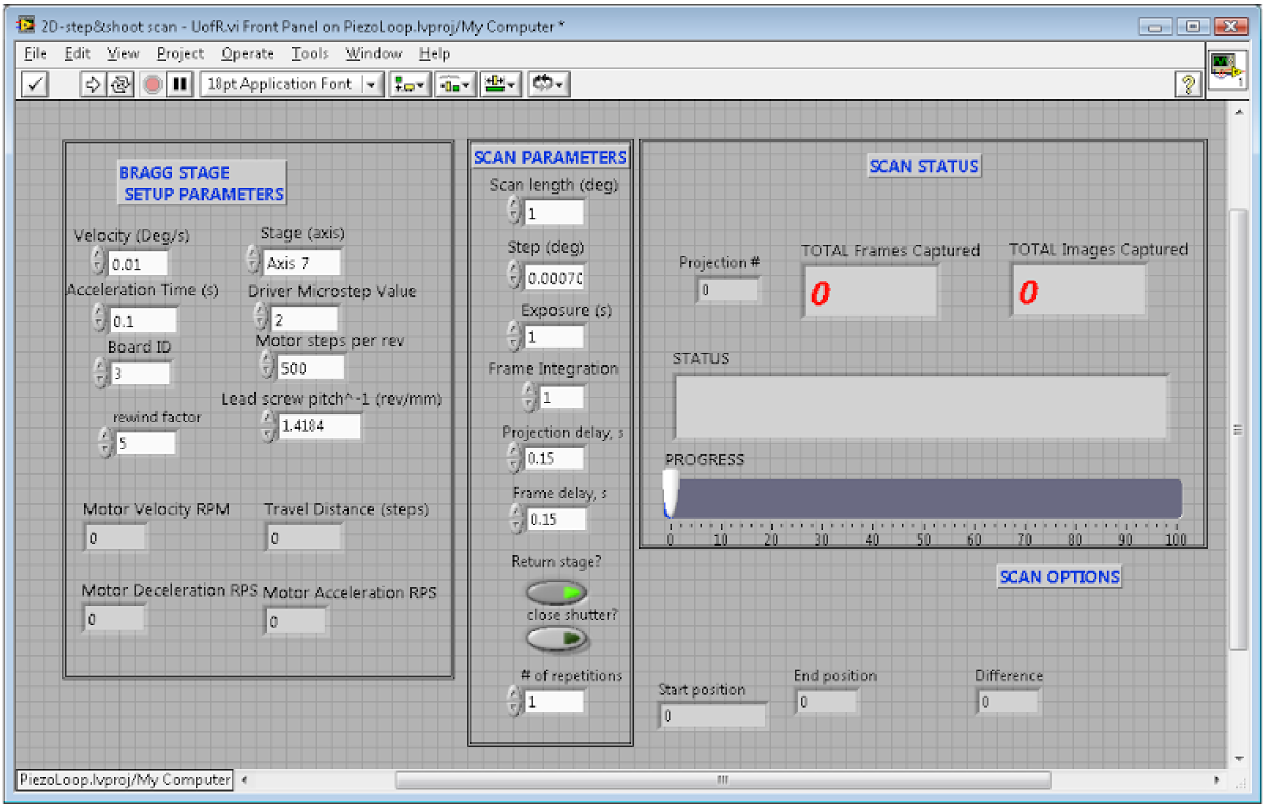

2D-snap&shoot scan Labview vi for controlling rocking curve scans

The Labview step&shoot vi should be run on electron4 in tandem with the HCImageLive which actually controls the camera running on WKS-000771 which runs the camera. This HCImageLive must absolutely be configured and running before any scans can be started. In the Capture pane (right side of canvas pane in the standard desktop view) there is section near the top called Camera Control that lets you set the exposure. That should never be set to 1s or greater, but anything up to 999 ms should be ok. This value should agree with what is set in the step&shoot vi under Exposure (middle panel). Similarly there should be agreement between frame integration and the integration setting in the camera gui. The Projection Delay and Frame Delay values of 150 ms are magic values that allow enough time for the camera controller to complete all of its operations.

Before starting the scan, be sure to go to the camera controller under the Trigger Modes panel, set the Capture Mode to “external edge” so that it is properly triggered by the Labview gui. To select the output image sequence, go to the Sequence pane in the camera controller and select AutoSave, then press the fat button to the right of it. Here you can set the output format (select TIFF), and the output directory, and the output prefix, and the sequence index start value. The file names are easier to sort if the “leading zeros” option on the sequence index values is selected. Before starting a scan, you need to compute how many steps the scan will take, and enter this value in the “End Frame” box, otherwise the program will not know when the scan is done and may stop prematurely. As soon as you are ready to start a scan, go to the Sequence pane in the camera controller and press Start after all of the configuration settings are in place. After this, you are ready to go to the scan Labview program and start the vi.

Logging of beamline conditions info

Programming staff here wrote a special script for us so we could automatically read and log some values related to the live state of the X-ray beam and beamline. This script runs on the Linux host (opi1128-003) and is called 05B1-1_Dump.sh, located in directory ~/URegina_201608 under the user bmit. The script appends information to a plain text file called 05B1-1_VarOutput.txt in the same directory. Here is a sample of the output that is written to this file. The meaning of each of these fields will be detailed in a later section of this logbook.

```
********************************************************
** BMIT BM (05B1-1) PV Dump - 2016/08/23 ...
********************************************************

WIG1405-01:systemTime          Tue Aug 23 18:35:48 2016
PCT1402-01:mA:fbk              191.939
SMTR1605-1-B10-10:Energy:curr  20.0719
SMTR1605-1-B10-10:Energy:curr:enc 19.9942
IOCH1605-B10-01:current:fbk    2.3069e-12
SMTR1605-1-B10-10:deg:sp       -9.2569
SMTR1605-1-B10-10:BraggAngle:fbk -9.29322
PFIL1605-1-B10-01:curr:material Aluminum
PFIL1605-1-B10-01:curr:actualThk 0.110338
PFIL1605-1-B10-02:curr:material none
PFIL1605-1-B10-02:curr:actualThk 0
PFIL1605-1-B10-03:curr:material none
PFIL1605-1-B10-03:curr:actualThk 0
SMTR1605-1-B10-03:mm:fbk       -17.3465
SMTR1605-1-B10-04:mm:fbk       13.3465
SMTR1605-1-B10-01:mm:fbk       1.9025
SMTR1605-1-B10-02:mm:fbk       -1.9015
```

First scan of UC45-X*

*X is equal to 5

August 24, 2016 [rtj, ns]
Diamond orientation is set such that the words “Threaded” are in the 12:00 position as viewed from upstream. The current in the ion chamber is 70 nA. We used the Pitch control gui to search for the 2,2,0 reflection and found it within 0.2 deg of nominal, just using the camera in internal trigger mode. We have good exposure using a camera shutter time of 990 ms, with the camera gain set to 15. Nazarin found a good focus in the camera image by tweaking the lever on the right side of the box labeled AA-40 (Hamamatsu Power Supply).

The camera is Hamamatsu AA-60, scintillator C9300-124. The following specs correspond to the camera

- field of view: 36mm x 24mm
- effective pixel size: 9um
- energy range: 3-30 keV
- readout speed: 2.5 frames/s
- scintillator material: P43 (Gd_20_2S:Tb) 10 microns thick

The edges of the rocking curve scan were at 0.237 deg and 0.184 deg, a difference of 940 urad. We decided to do 75 steps of minimum step size 0.000706 deg (limiting size of step for this Pitch motor).

scan number	theta range (deg)	no. steps	step size (urad)	image prefix
1	(0.184, 0.237)	74	12.3	UC45-X-2-1
2	“	“	“	UC45-X-2-1
3	“	“	“	UC45-X-3-1
4	“	“	“	UC45-X-4-1

Visually, I can see that there is a significant amount of motion of the diffraction band with a time scale on the order of 1 second. I wonder if there are higher frequencies present as well. This is something we will need to study if we want to optimize our rocking curve resolution. I now copy these results from CLS to UConn so I can run an analysis of the scans.

To copy data from CLS to UConn, I tried to set up a globus endpoint on BMIT-NI-2 workstation. I was not able to install the personal globus endpoint on this machine with default privileges, but Adam knew the Administrator password and he allowed

CLS machine name: BMIT-BM (setup key 71be21d4-2ce8-47dd-9502-c136833fc1e0)

For the next 4 scans (5-8) we turned down the air handler flow inside the hutch and repeated the rocking curves. We did this because we hoped

scan number	theta range (deg)	no. steps	step size (urad)	image prefix
5	(0.184, 0.237)	74	12.3	UC45-X-5-1
6	“	“	“	UC45-X-6-1
7	“	“	“	UC45-X-7-1
8	“	“	“	UC45-X-8-1

I transferred the initial scan data to UConn and installed them on the staging disk /export/data0 on grinch. The files have names like UC45-X-1-1_NNNNN.tif where NNNNN is the step index in the scan. I skipped forward to scan number 11 to reduce the number of redundant fields in the filename.

scan number	theta range (deg)	no. steps	step size (urad)	image prefix
11	(0.213, 0.265)	74	12.3	UC45-X-11
12	“	“	“	UC45-X-12
13	“	“	“	UC45-X-13
14	“	“	“	UC45-X-14
15*	“	“	“	UC45-X-15
16*	“	“	“	UC45-X-16

*Scans 11-14 above were taken under identical conditions, with projection delay = 0.15 seconds whereas scans 15-16 were taken with the projection delay increased to 3 seconds.

For the next set of scans, we changed the settings on the Pitch motor to give an order of magnitude more microsteps per step. This increases the resolution of the motor to be 1.23 urad per increment in the motor position. To match the new setting on the controller, we need on the Pitch controller gui (and in the step&shoot gui) to set the “Driver Microstep Value” from 2 to 20. The new scan length was reduced to 0.0350 deg (600 urad) and then the step resolution increased to the next setting, in order to see if there is substructure to these rocking curve peaks which might give us hints as to the origin of the excess width.

scan number	theta range (deg)	no. steps	step size (urad)	image prefix
17	(0.235, 0.270)	498	1.23	UC45-X-17

Diagnosing the wide rocking curve peaks

One possible source for the motion in the diffraction band observed in the rocking curve measurements of UC45-X is that the beam is hitting the monochromator at an angle which is changing over time. If the incident angle of the beam w.r.t. the crystal planes of the first monochromator is changing over the course of a rocking curve measurement the diffraction band would move as well. We would like to measure the magnitude of these oscillations in beam angle to see how large of an effect it is. We put a molybdenum filter before the monochromator and moved the diamond away from its diffraction edge so that it would not diffract into the 2θ detector. Then we found the middle of the diffraction edge of the molybdenum (which has a width of 10eV) and narrowed the beam slits (before the mono) so that there was a 0.2mm slit centered in the vertical axis of the beam. Narrowing the slits selects only a small range of k values from the beam, we are limited by the smallest step size of the shutter motors (0.1mm). Beam was brought into the hutch and we watched the amplitude in the Piezo Feedback LabView GUI and measured the peak-to-peak oscillation of the amplitude to be a few percent, which represents roughly 0.2eV. The energy dispersion as a function of angular spread was calculated as shown below for molybdenum.

$$q = k * \sin\theta$$
$$k = q / \sin\theta$$
$$dk/d\theta = q / \sin\theta * \tan\theta = 0.158 \text{ eV} / \mu\text{rad}$$

The dk value is very small because of how narrow the beam slits are and the leading order variations over time of the amplitude seen in the Piezo Feedback GUI should represent the beam’s change in incident angle over time. We would have had to have seen a much larger oscillation in transmission amplitude to explain the motion in the diffraction band which was an order of magnitude larger for the UC45-X measurements. We later discovered that these variations were present even without beam in the hutch, meaning that the source was simply electronic noise.

Corrections for off-center pitch sweeps

It's likely that the diamond is not in the center of rotation of the goniometer, especially considering that no attempt was previously made to center it. Typically this is done by placing a needle in the goni mount and then sighting the tip of the needle (with a surveyor's scope) while rotating and adjusting the stages until the needle does not precess. This particular setup is limited by how much movement the mount has in the y-coordinate and so we will chose to take this offset out within the software. To better understand the effect this has on the rocking curve

Camera ix pixel start: 2098
Width: 1176 pixels
Camera iy pixel start: 576
Width: 2024 pixels

Rocking Curve Images of UC45-X

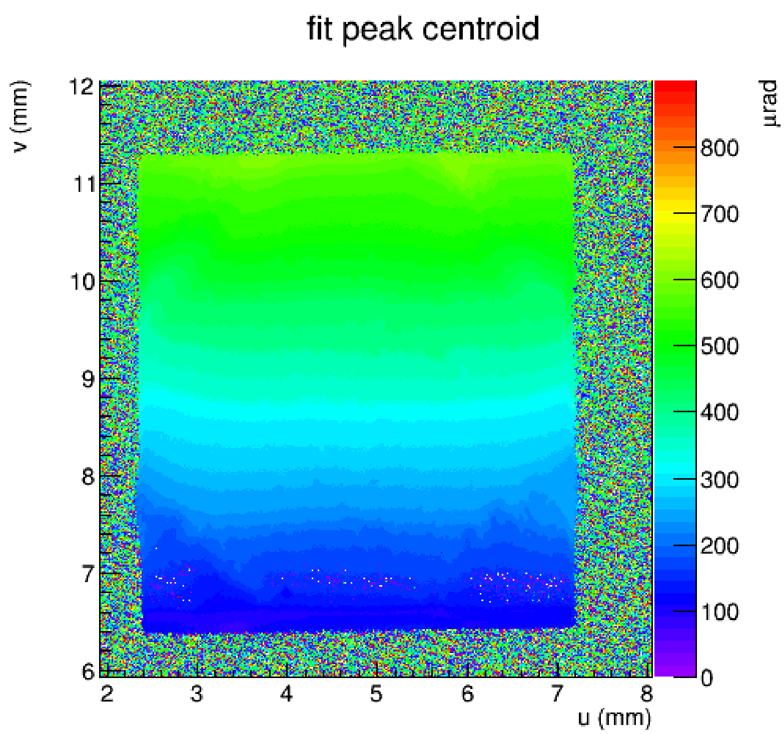

Figure: Image of rocking curve data analyzed for UC45-X-1_001. The bin values in the z axis are the mu parameters of the fit made over the entire run for each individual pixel of the diamond seen by the camera.

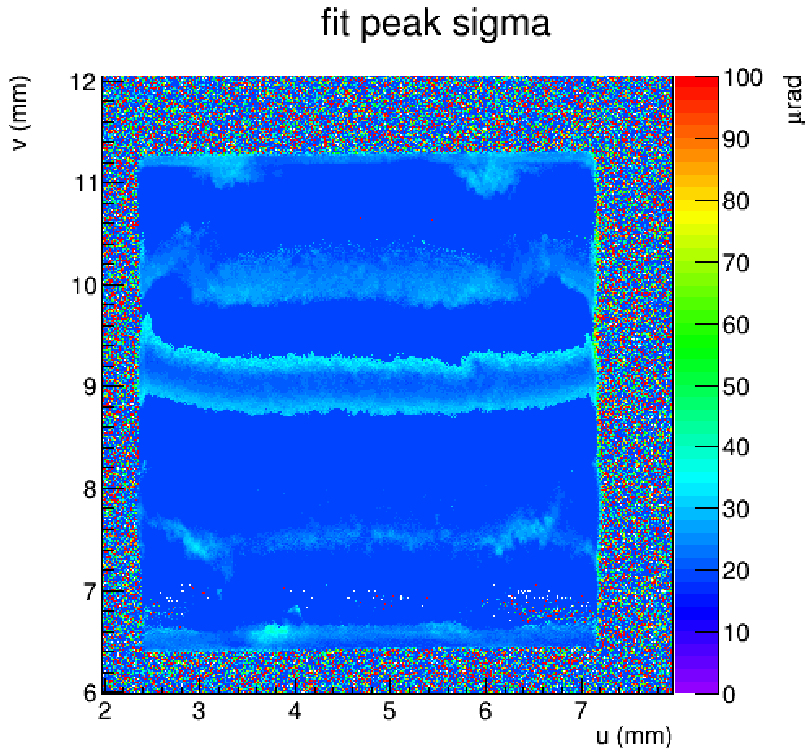

Figure: Image of rocking curve data analyzed for UC45-X-1_001. The bin values in the z axis are the sigma parameters of the fit made over the entire run for each individual pixel of the diamond seen by the camera

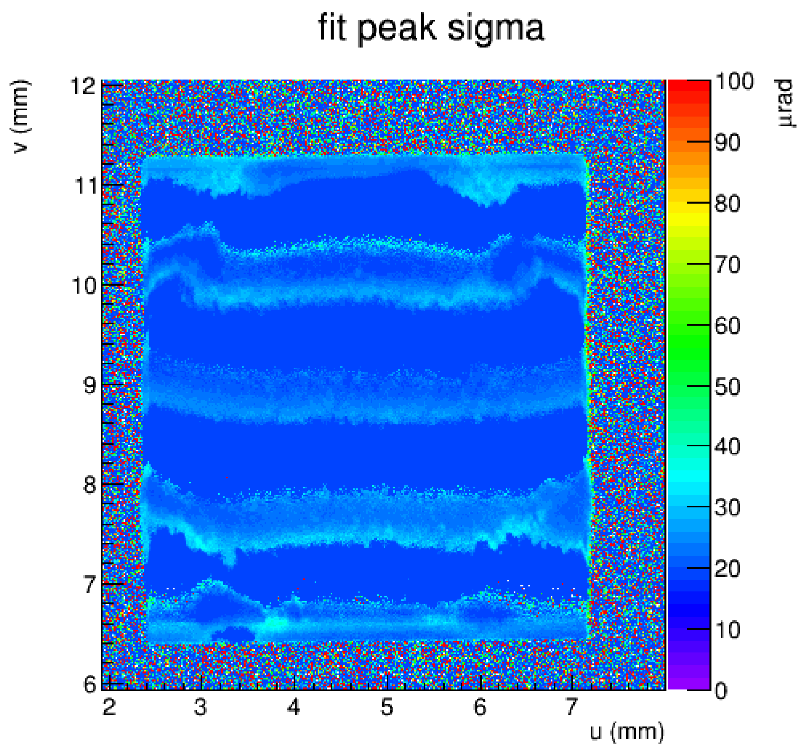

Figure: Image of rocking curve data analyzed for UC45-X-2_001. The bin values in the z axis are the sigma parameters of the fit made over the entire run for each individual pixel of the diamond seen by the camera

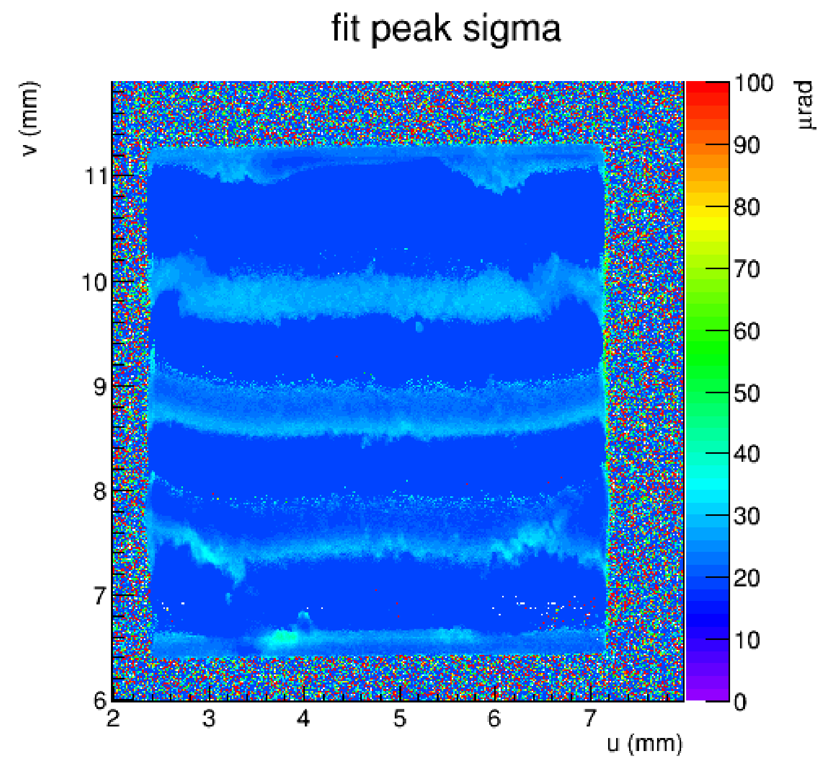

Figure: Image of rocking curve data analyzed for UC45-X-3_001. The bin values in the z axis are the sigma parameters of the fit made over the entire run for each individual pixel of the diamond seen by the camera

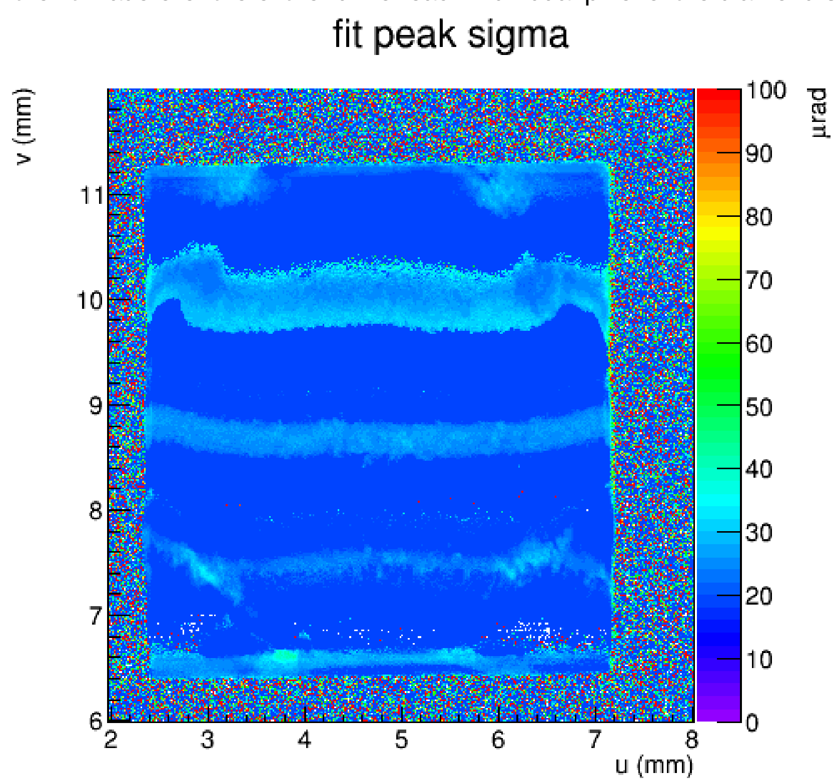

Figure: Image of rocking curve data analyzed for UC45-X-4_001. The bin values in the z axis are the sigma parameters of the fit made over the entire run for each individual pixel of the diamond seen by the camera

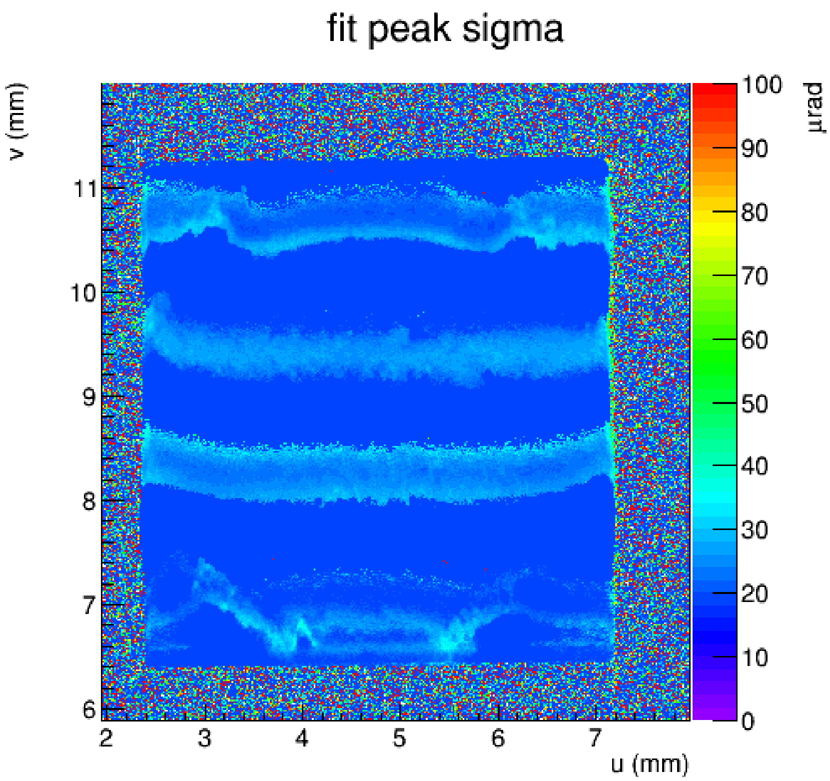

Figure: Image of rocking curve data analyzed for UC45-X-5_001. The bin values in the z axis are the sigma parameters of the fit made over the entire run for each individual pixel of the diamond seen by the camera

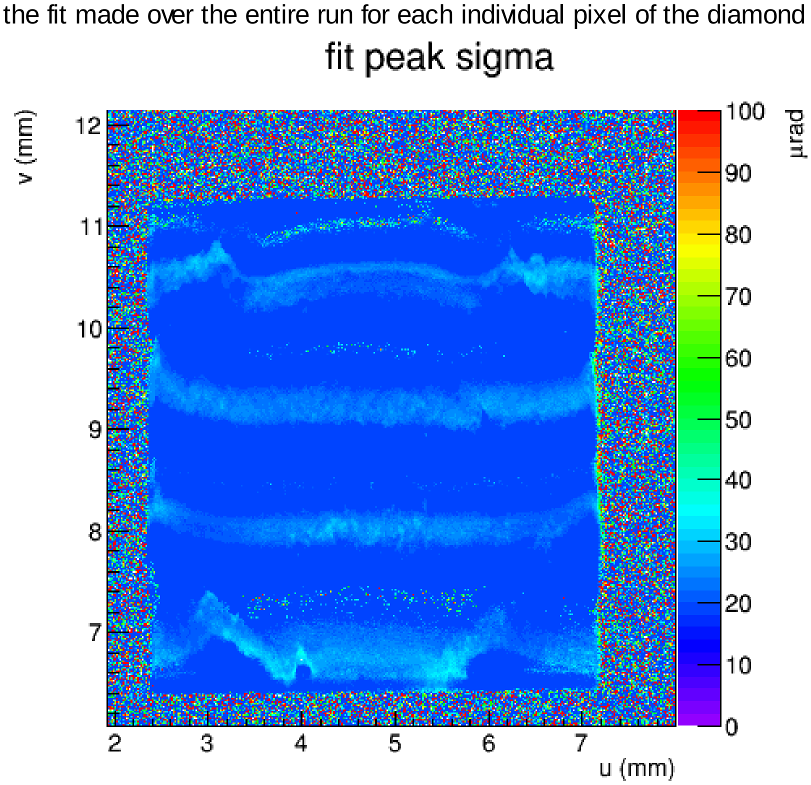

Figure: Image of rocking curve data analyzed for UC45-X-6_001. The bin values in the z axis are the sigma parameters of the fit made over the entire run for each individual pixel of the diamond seen by the camera

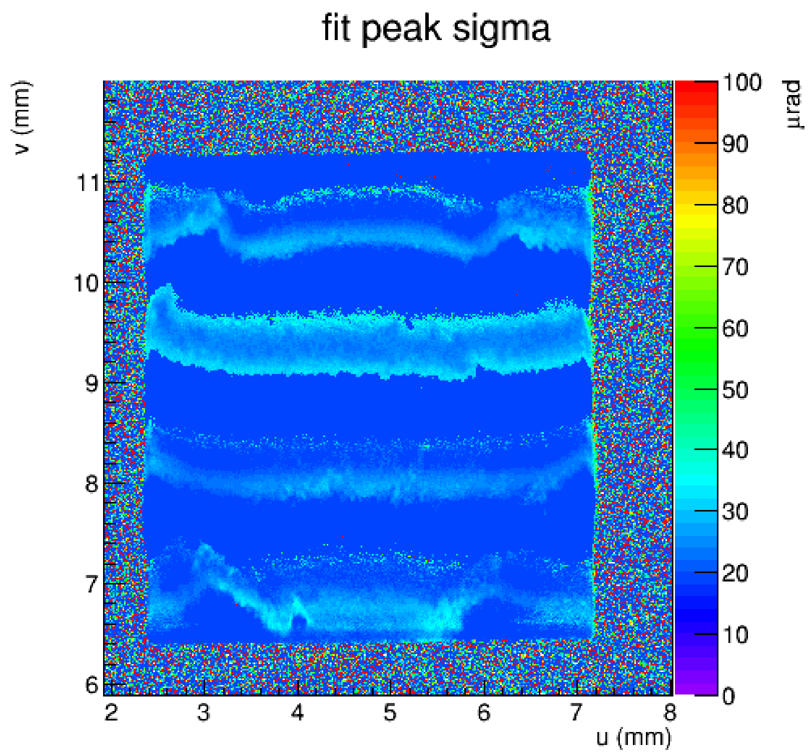

Figure: Image of rocking curve data analyzed for UC45-X-7_001. The bin values in the z axis are the sigma parameters of the fit made over the entire run for each individual pixel of the diamond seen by the camera

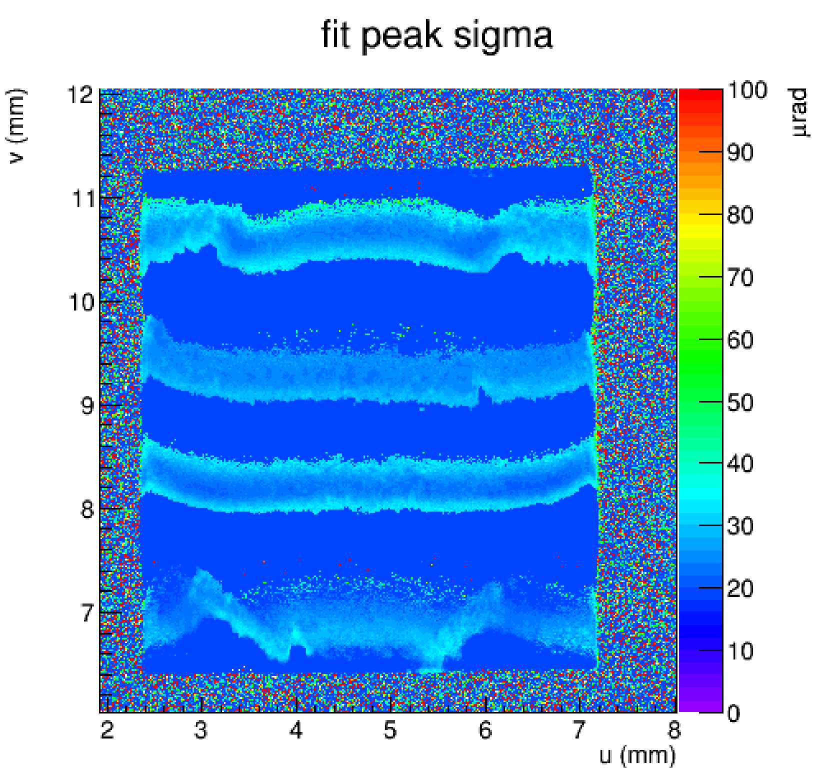

Figure: Image of rocking curve data analyzed for UC45-X-8_001. The bin values in the z axis are the sigma parameters of the fit made over the entire run for each individual pixel of the diamond seen by the camera

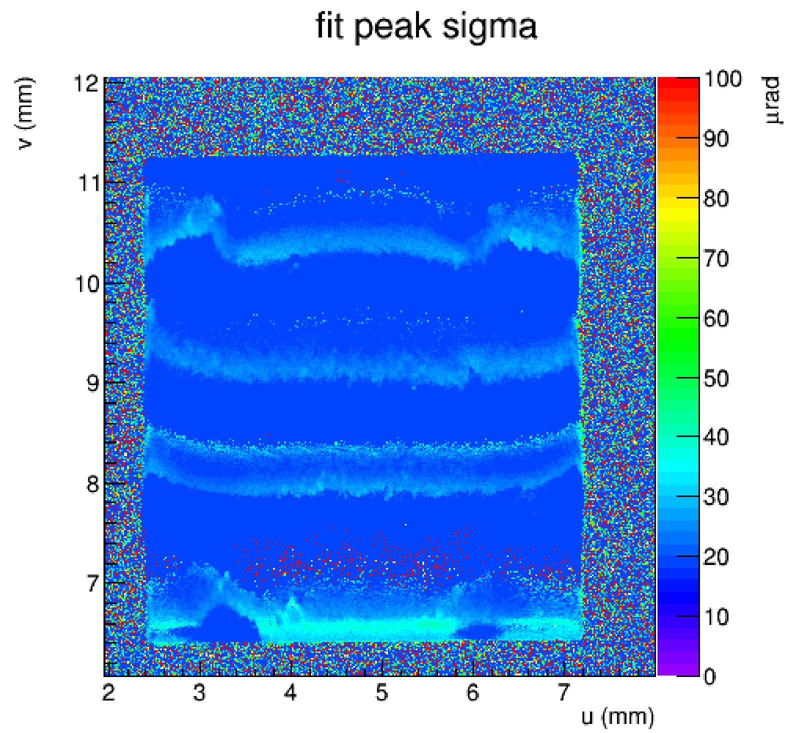

Figure: Image of rocking curve data analyzed for UC45-X_011. The bin values in the z axis are the sigma parameters of the fit made over the entire run for each individual pixel of the diamond seen by the camera

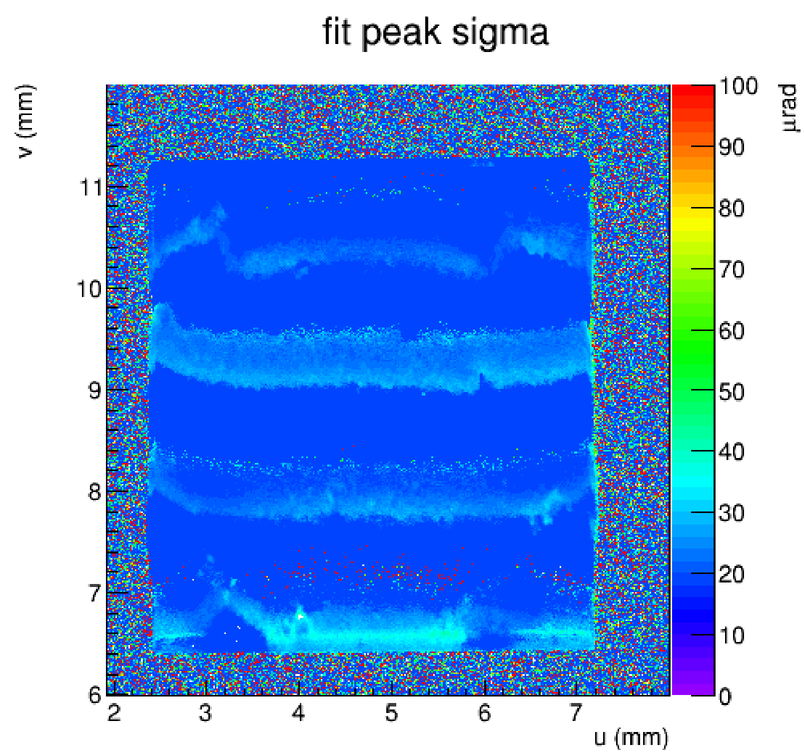

Figure: Image of rocking curve data analyzed for UC45-X_012. The bin values in the z axis are the sigma parameters of the fit made over the entire run for each individual pixel of the diamond seen by the camera

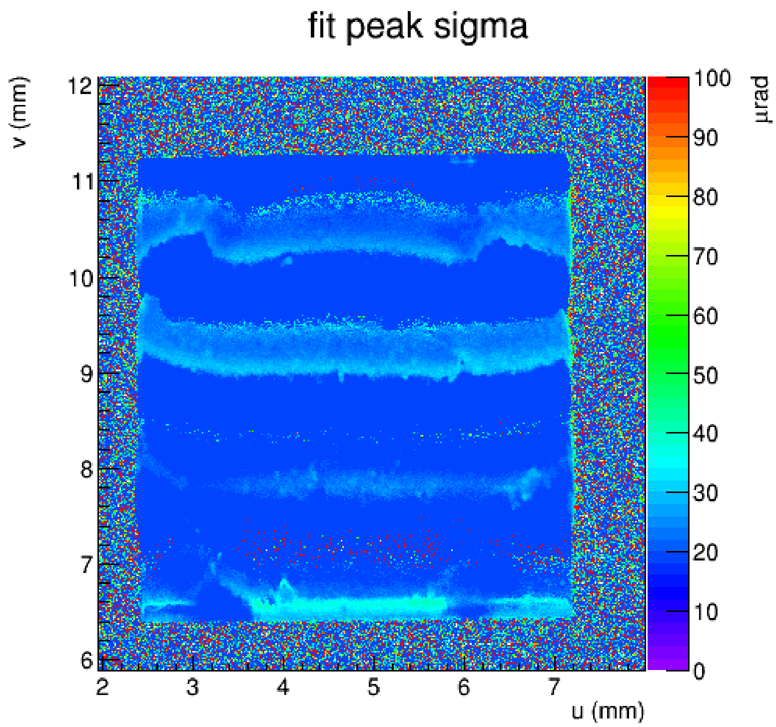

Figure: Image of rocking curve data analyzed for UC45-X_013. The bin values in the z axis are the sigma parameters of the fit made over the entire run for each individual pixel of the diamond seen by the camera

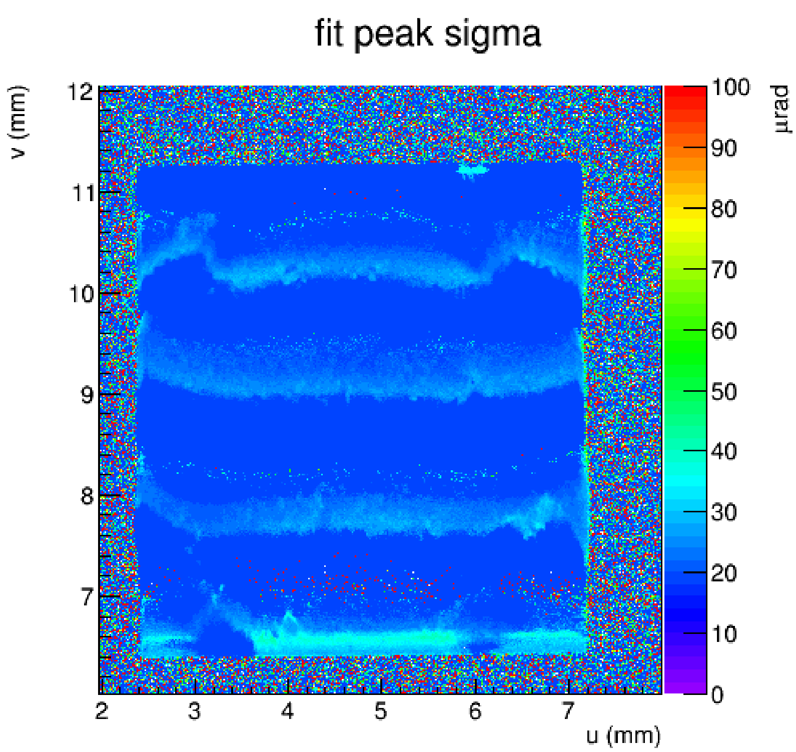

Figure: Image of rocking curve data analyzed for UC45-X_014. The bin values in the z axis are the sigma parameters of the fit made over the entire run for each individual pixel of the diamond seen by the camera

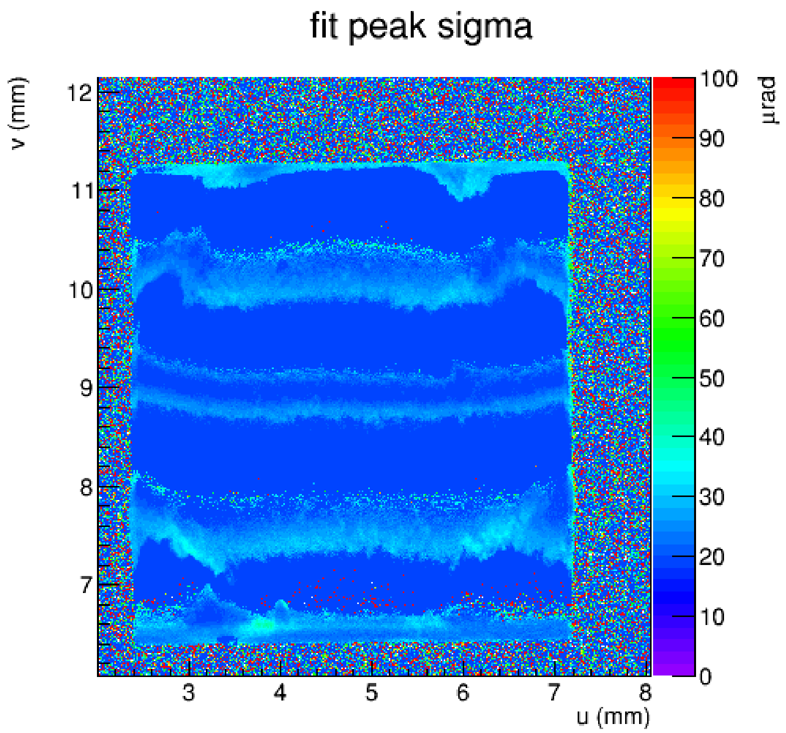

Figure: Image of rocking curve data analyzed for UC45-X_015. The bin values in the z axis are the sigma parameters of the fit made over the entire run for each individual pixel of the diamond seen by the camera

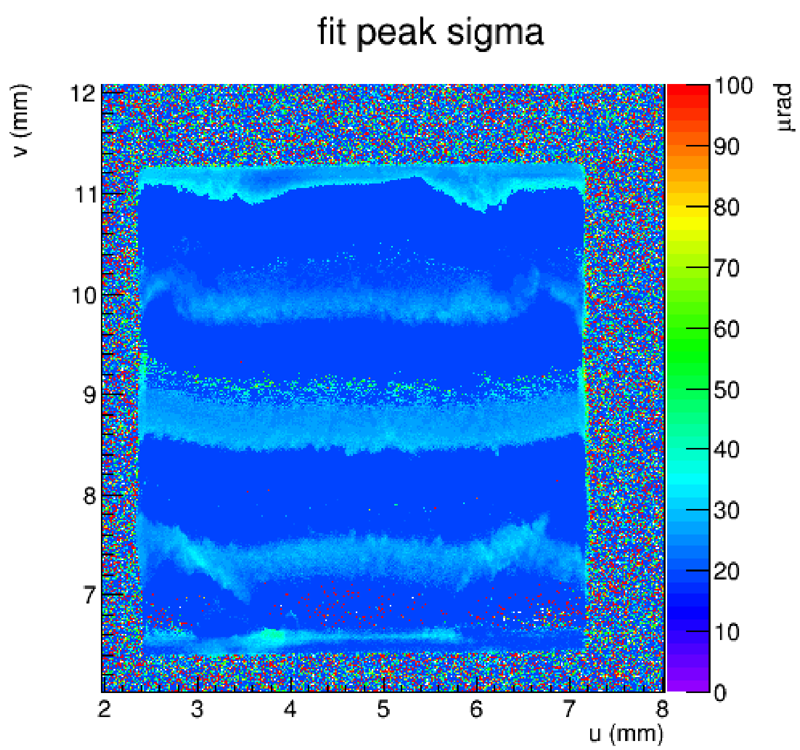

Figure: Image of rocking curve data analyzed for UC45-X_016. The bin values in the z axis are the sigma parameters of the fit made over the entire run for each individual pixel of the diamond seen by the camera.

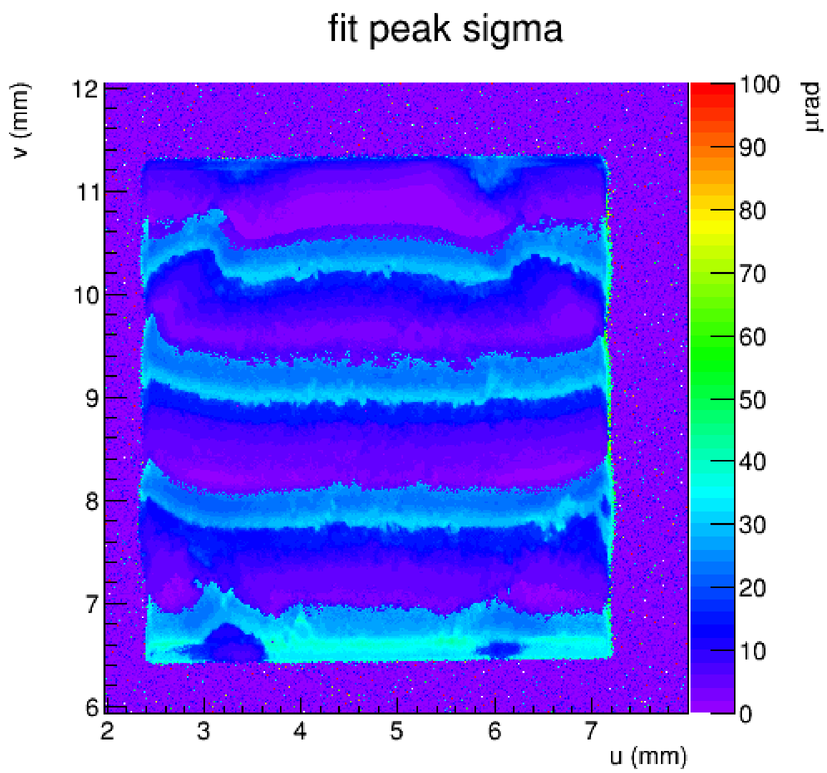

Figure: Image of rocking curve data analyzed for UC45-X_017. The bin values in the z axis are the sigma parameters of the fit made over the entire run for each individual pixel of the diamond seen by the camera

Systematics studies of banded topographs

August 25, 18:00, [rtj]

We did a new set of scans to test some ideas of what is causing the banded structure in the above topographs. For these scans, we reset the Projection Delay to its default value of 0.15s, as this did not seem to have any observable effect on the topographs. For scan 18, we reduced the holding current on the stepper motor for the Pitch angle from its default value 28% to its minimum value 10% of the stepping current.

scan number	theta range (deg)	no. steps	step size (urad)	image prefix
18*	(0.282, 0.317)	49	12.3	UC45-X-18
19**	(0.283, 0.318)	49	12.3	UC45-X-19

* scan 18 was taken with the motor holding current reduced from 30% to 10%

** scan 19 was taken with the motor holding current increased to 55% from 30%

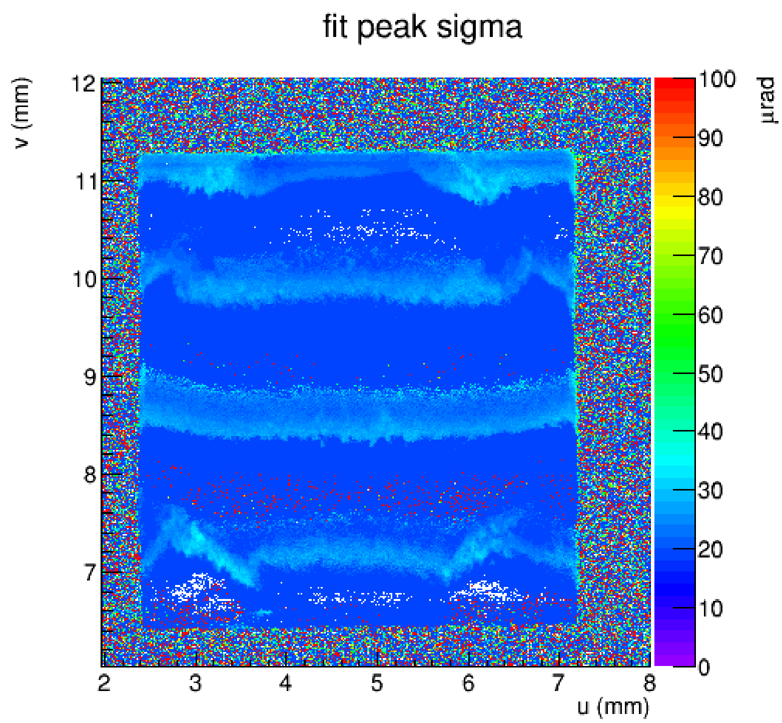

Figure: Image of rocking curve data analyzed for UC45-X_018. The bin values in the z axis are the sigma parameters of the fit made over the entire run for each individual pixel of the diamond seen by the camera. This run was completed with the holding current of the theta motor reduced from 30% to 10%.

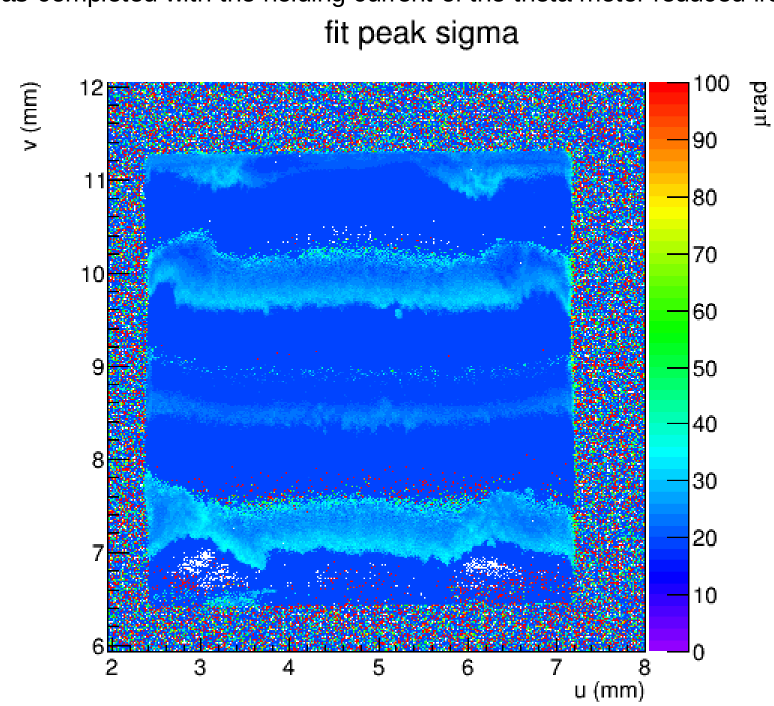

Figure: Image of rocking curve data analyzed for UC45-X_018. The bin values in the z axis are the sigma parameters of the fit made over the entire run for each individual pixel of the diamond seen by the camera. This run was completed with the holding current of the theta motor reduced from 30% to 55%.

Next we rotated the target holder by 90 degrees in chi. The words “Threaded” are now at position 3:00 as viewed from upstream of the target. We used a fluorescent screen to find the reflection, and then ran a new scan, which I assigned to number 20.

scan number	theta range (deg)	no. steps	step size (urad)	image prefix
20	(1.444, 1.472)	39	12.3	UC45-X-20
21*	(1.444, 1.472)	39	12.3	UC45-X-21
22**	(1.444, 1.472)	39	12.3	UC45-X-22

* scan 21 was a repeat of scan 20, except that we increased Frame Integration to 3 to increase the signal-to-noise ratio. This scan was taken toward the end of a spill, so the intensity was quite low.

** scan 22 was a repeat of scan 20, except that we increased Frame Integration to 2 to decrease the signal-to-noise ratio, because scan 21 was showing saturation near the bottom of the image.

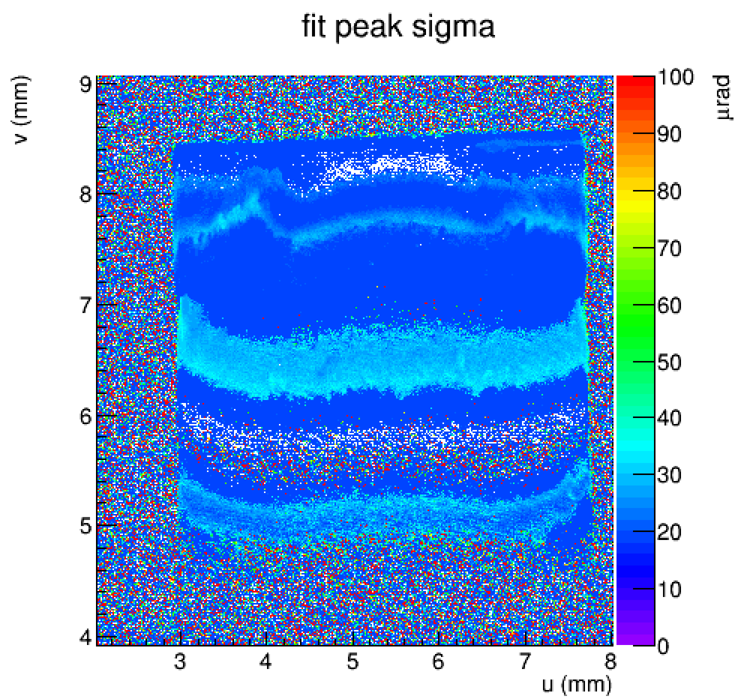

Figure: Image of rocking curve data analyzed for UC45-X_020. The bin values in the z axis are the sigma parameters of the fit made over the entire run for each individual pixel of the diamond seen by the camera.

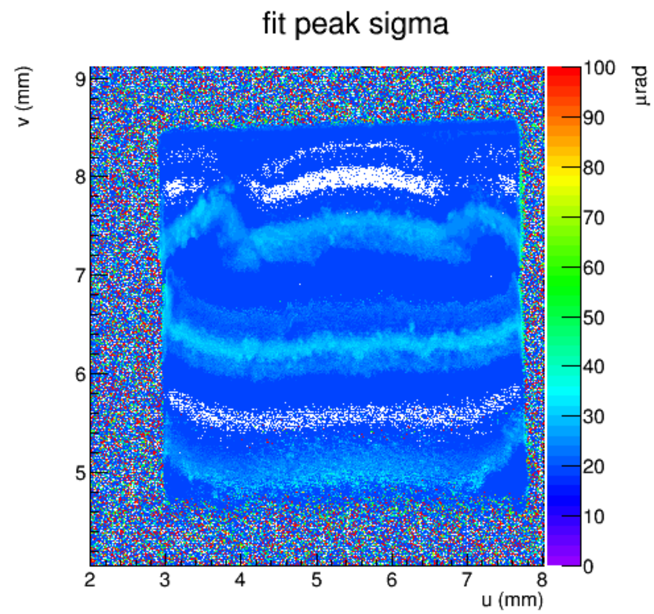

Figure: Image of rocking curve data analyzed for UC45-X_021. The bin values in the z axis are the sigma parameters of the fit made over the entire run for each individual pixel of the diamond seen by the camera.

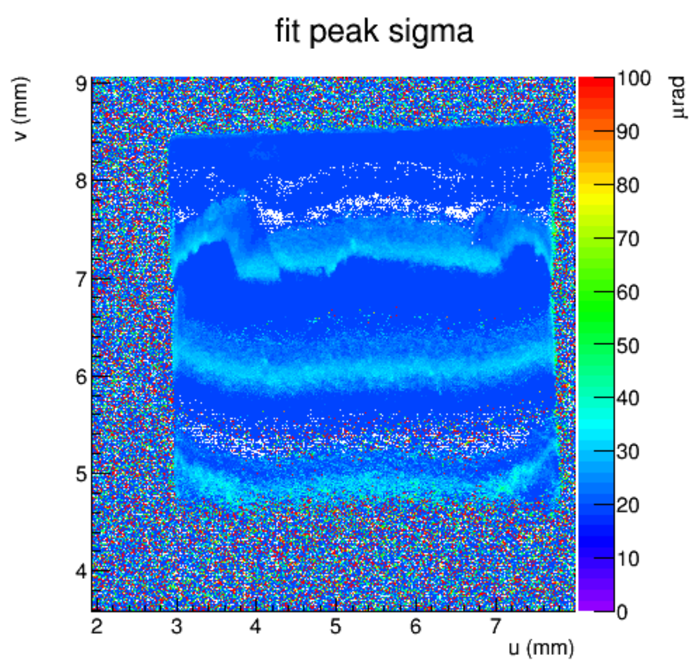

Figure: Image of rocking curve data analyzed for UC45-X_022. The bin values in the z axis are the sigma parameters of the fit made over the entire run for each individual pixel of the diamond seen by the camera.

Hypothesis of banded structures in UC45-X

August 26, 8:00am [BJP,RTJ]

A possible explanation for the bands present in all the rocking curve measurements of UC45-X is that they are caused by the pendellosung effect. The pendellosung effect in transmission-mode diffraction is where the intensity of the flux in the bulk of the crystal oscillates between the two modes of X-rays propagating through the diamond, one with direction Kinc and the other with direction Kref, like a pair of coupled oscillators (see the image below).

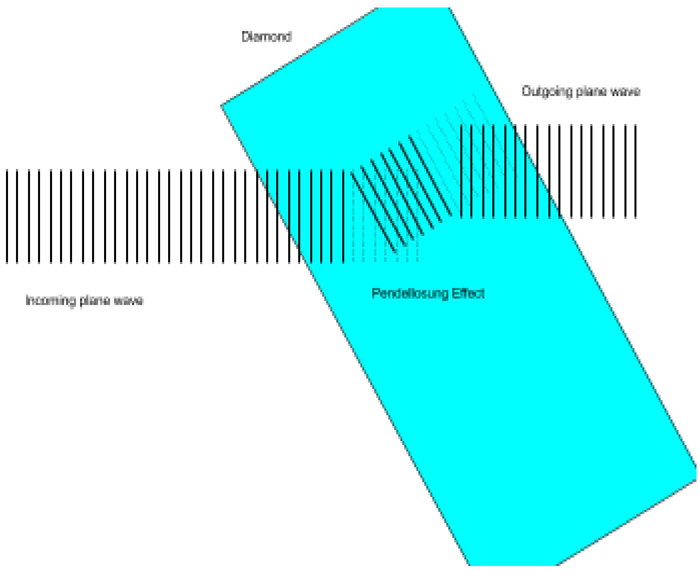

Figure: Illustration of the Pendellosung Effect.

In the figure above, the incoming plane wave is initially perpendicular to the lab floor. As it penetrates the diamond it is diffracted and directed towards 2θ, the perpendicular mode of the beam extinguishes to zero amplitude just as the diffracted beam reaches a maximum. The beam may again be diffracted within the crystal and brought back to the perpendicular orientation. This oscillation may occur many times within the crystal and the resulting output beam will either be directed towards or away from 2θ. If the beam originally had zero dispersion, the resulting pattern seen by the detector over a rocking curve scan would look like the following.

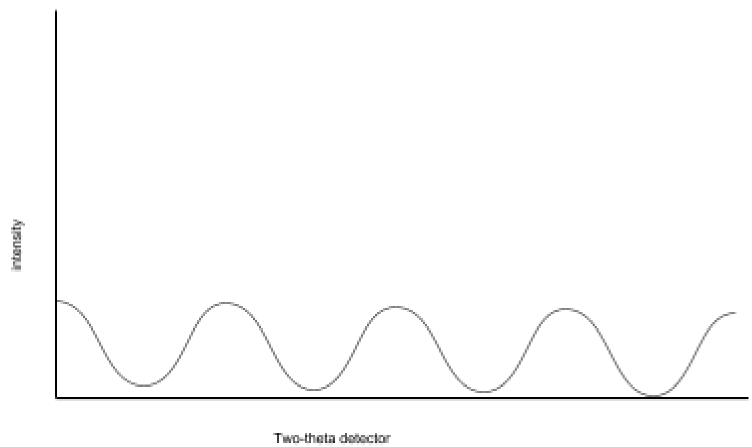

Figure: Simple illustration of the intensity profile seen across a column of pixels of the two-theta detector for a rocking curve measurement where the crystal undergoes the Pendellosung Effect.

Because the beam is not dispersion matched with the diamond, we have to rock the diamond through a large range of angle to cover the entire area of the crystal. As we rock through theta, narrow bands of the diamond diffract and are modulated by the Pendellosung Effect. We believe that this effect is shaping the inherent rocking curve width of the diamond, producing the oscillatory pattern seen in all the measurements so far.

To test this idea, we are going to change the beam optics so that we are down-bouncing instead of up-bouncing. All measurements up to this point have been conducted with the beamline in the up-bounce configuration which is not dispersion matched. By switching to an down-bounce configuration, the beam will be better dispersion matched to the diamond crystal. This means that a much larger percentage of the diamond area will diffract and fewer steps in theta will be required to measure the entire rocking curve. Our prediction is that since we will be diffracting over a larger area of the crystal the bands seen in the above measurements will widen. Hopefully they will be so wide that the rocking curve of the diamond lives within a single band. The bands alternate between regions of low rocking curve width and high rocking curve width and we can adjust which one the diamond is centered in by tweaking the mono. We are currently repositioning the diamond mount and two-theta camera so that we achieve the geometry described above. An illustration of the up-bounce/down-bounce process is shown below.

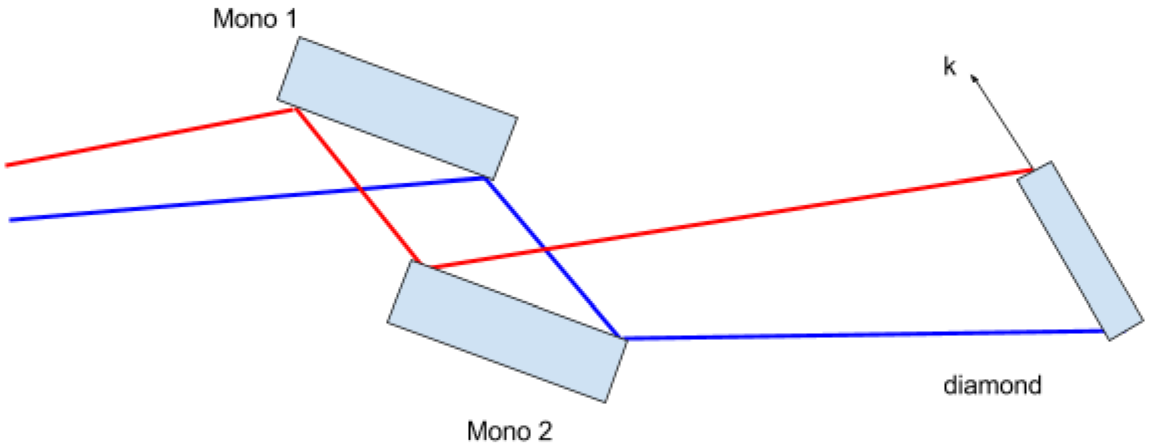

Figure Up-Bounce: Diagram of beamline optics and diamond diffraction in the up-bounce orientation

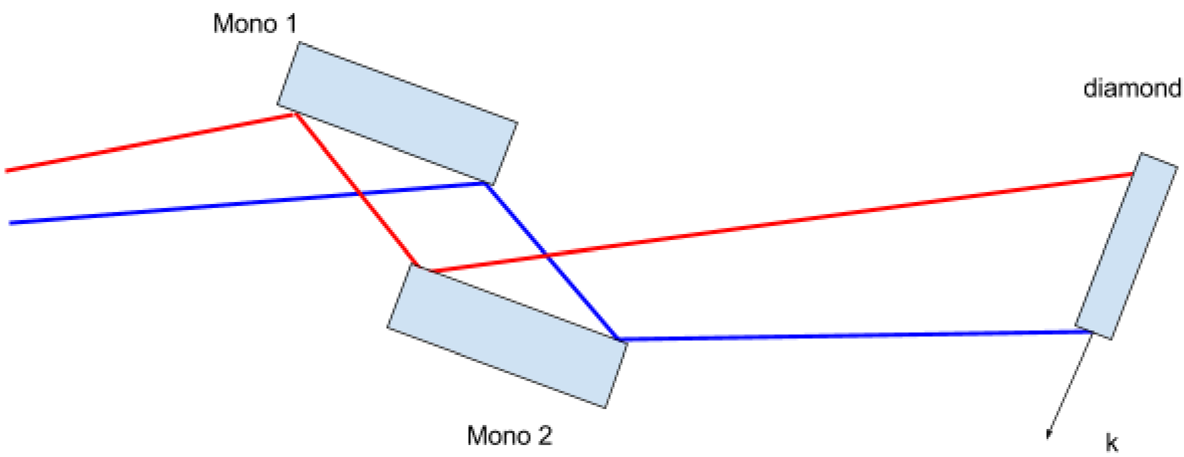

Figure Down-Bounce: Diagram of beamline optics and diamond diffraction in the up-bounce orientation

Scans of UC45-X in down-bounce geometry

We moved the camera to a position 30 degrees below the horizontal and tipped the diamond to 15 degrees past the vertical, with the chi orientation unchanged ("Threaded" at 3:00 viewed from upstream). We did a scan with the fluorescent screen and found the diffraction peak about 2 degrees away from the expected position. We then reset the cropping window in the camera frame to include only the region around the diamond image, took down the fluorescent screen, and started a new scan.

scan number	theta range (deg)	no. steps	step size (urad)	image prefix
23	(3.435, 3.448)	96	2.46	UC45-X-23

The following video shows a live view of the motion of the diffracted beam image in the down-bounce geometry while the hoop is stationary and nothing is supposed to be changing.

Watch the Diamond diffraction image dance.

The rocking curve topograph from scan 23 is shown in the figure below. Apart from broad pixels near the top and bottom edges of the crystal, the rocking curve peaks are narrow and relatively clean. One interpretation is that the “bands” are still present, but their apparent spacing has increased because of the partial cancellation between the dispersion of the beam and diamond diffraction slope (imperfect dispersion match, but much closer than before) which decreases the angular range needed to rock the entire crystal through the 2,2,0 peak.

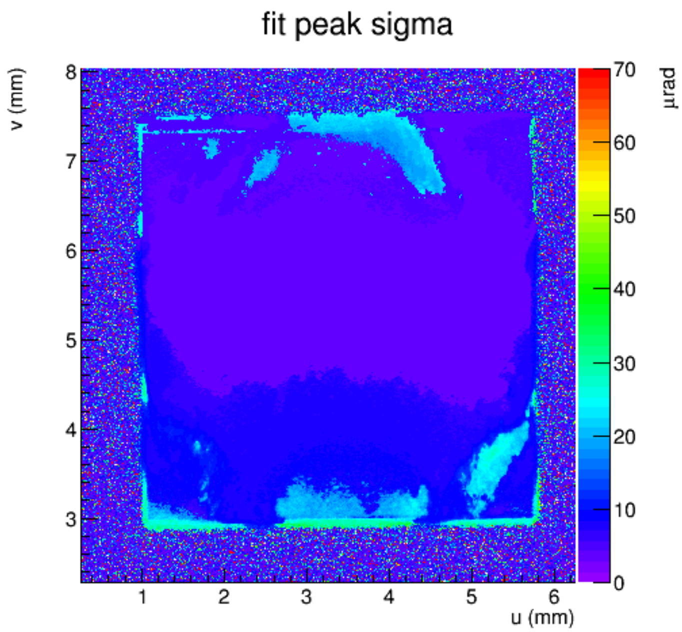

Figure: Image of rocking curve data analyzed for UC45-X_023. The bin values in the z axis are the sigma parameters of the fit made over the entire run for each individual pixel of the diamond seen by the camera.

To attempt to understand the causes for the big temporal variation, we replaced the light-weight pinch-mount fixture with a heavy-duty crystal holder assembly. The next 4 scans were taken with

scan number	theta range (deg)	no. steps	step size (urad)	image prefix
24	(0.863, 0.875)	85	2.46	UC45-X-24
25	(0.863, 0.875)	85	2.46	UC45-X-25

26	(0.863, 0.875)	85	2.46	UC45-X-26
27	(0.863, 0.875)	85	2.46	UC45-X-27

The rocking curve width color map images from the above scans are shown below.

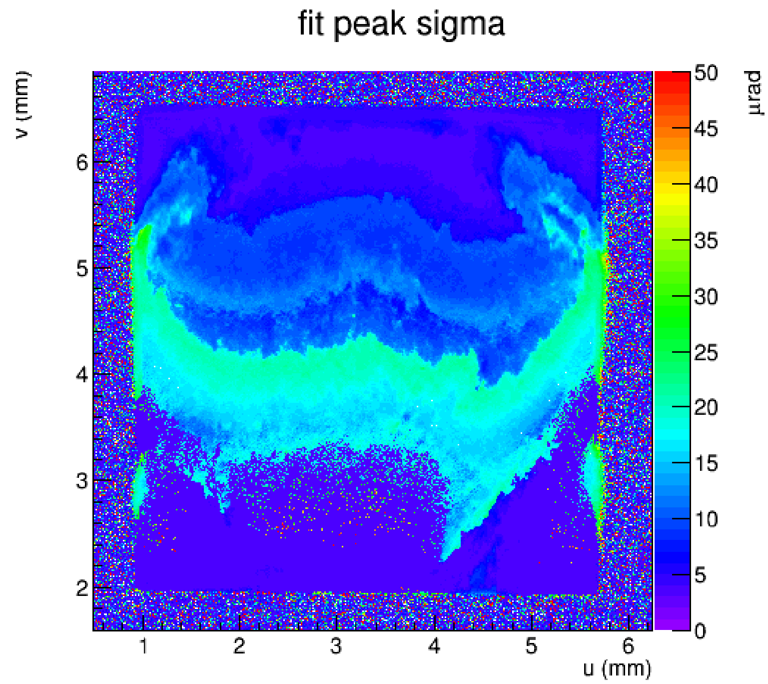

Figure: Image of rocking curve data analyzed for UC45-X_024. The bin values in the z axis are the sigma parameters of the fit made over the entire run for each individual pixel of the diamond seen by the camera.

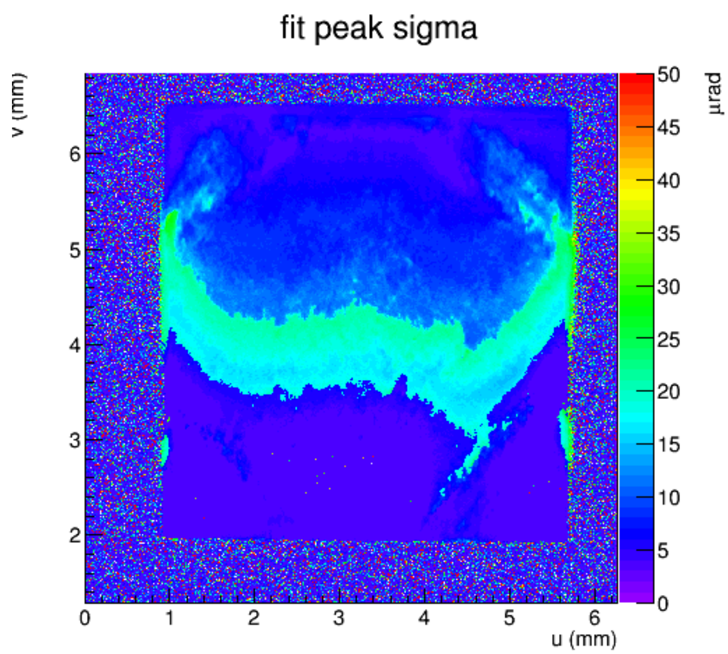

Figure: Image of rocking curve data analyzed for UC45-X_025. The bin values in the z axis are the sigma parameters of the fit made over the entire run for each individual pixel of the diamond seen by the camera.

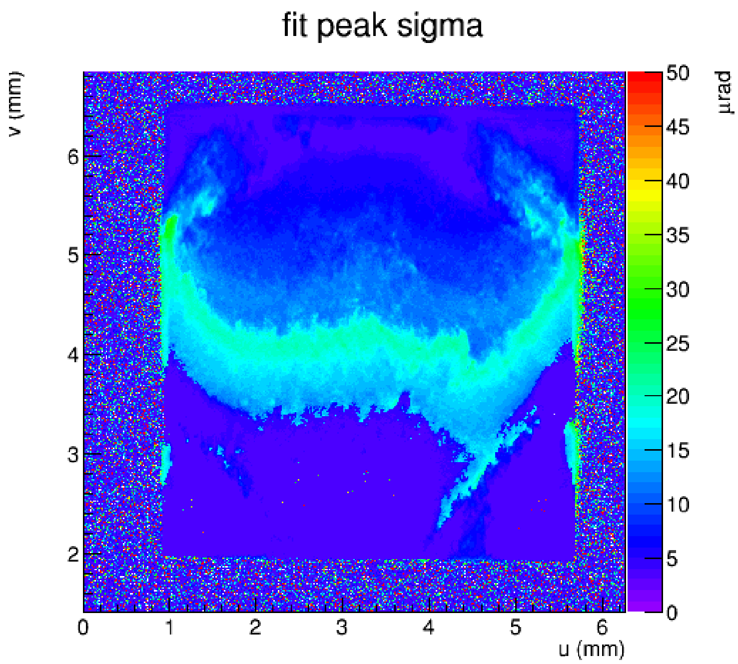

Figure: Image of rocking curve data analyzed for UC45-X_026. The bin values in the z axis are the sigma parameters of the fit made over the entire run for each individual pixel of the diamond seen by the camera.

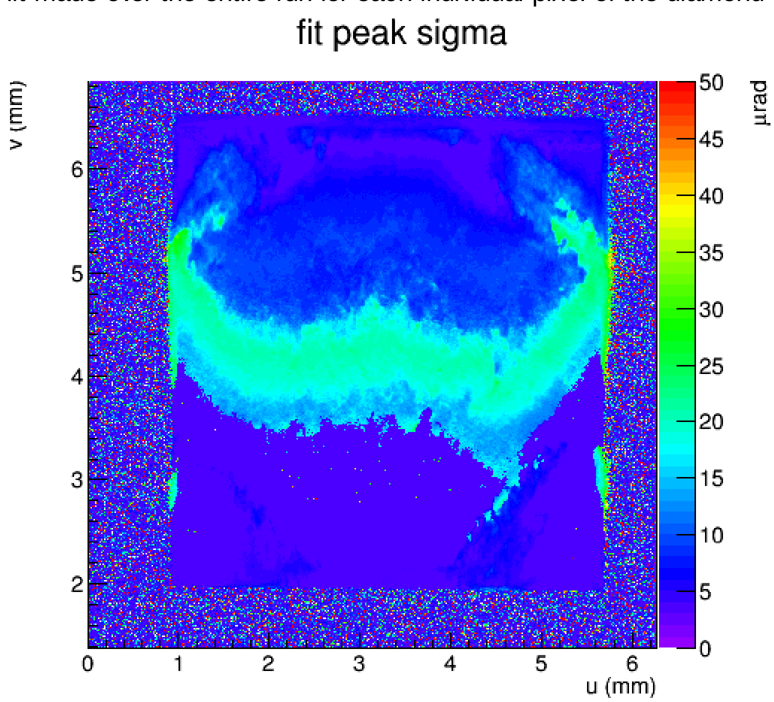

Figure: Image of rocking curve data analyzed for UC45-X_027. The bin values in the z axis are the sigma parameters of the fit made over the entire run for each individual pixel of the diamond seen by the camera.

Unfortunately, the band now appears right in the center of the diamond rocking curve topograph.

The full height of the crystal in terms of rocking curve angle is around 100 urad, which translates to 25 eV in the beam dispersion. so I guess that if I shift the mono energy by something close to 25 eV, it should be possible to move the band off the top of the crystal and leave the crystal exposed to the clear narrow-peak region between the bands where the intrinsic rocking curve width of the crystal is seen.

scan number	theta range (deg)	no. steps	step size (urad)	image prefix
28	(0.000, 0.0140)	99	2.46	UC45-X-28

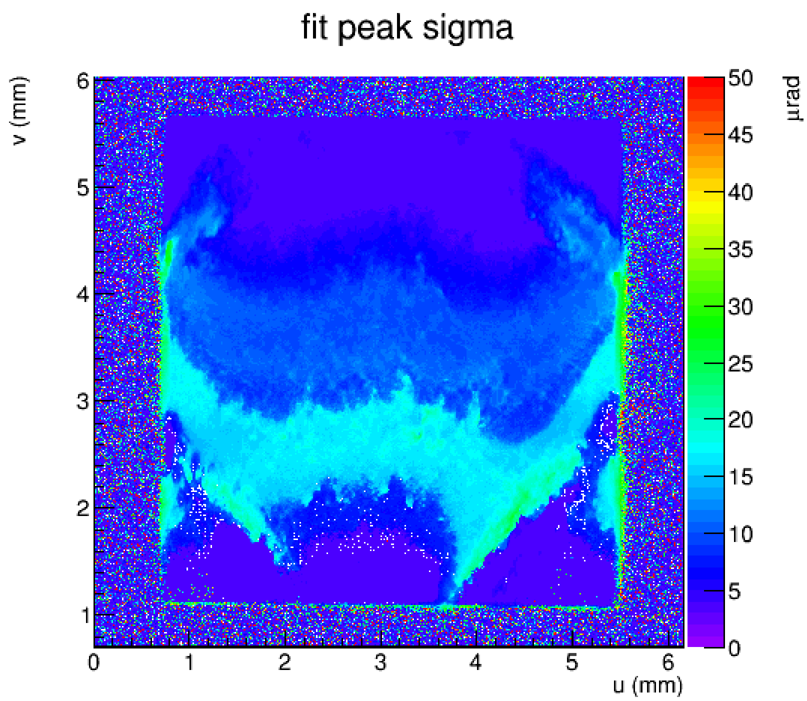

Figure: Image of rocking curve data analyzed for UC45-X_028. The bin values in the z axis are the sigma parameters of the fit made over the entire run for each individual pixel of the diamond seen by the camera.

This image shows that the band has shifted, but only by 1/4 of the total height of the crystal. We try this same shift again, but by 75 eV this time, for a total of 100 eV. The results of this are shown in scan 29. Apparently this is too much of a change, as a new band seems to have moved into the diamond from the top. For scan 30, we back off by 40 eV, for a total of 60 eV from nominal 20 keV. The hope with this compromise is to push the two bands to the top and bottom edges of the diamond, and leave the central region free of these features which we believe are artifacts of the beamline instrumentation.

scan number	theta range (deg)	no. steps	step size (urad)	image prefix
29	(-0.052, -0.039)	93	2.46	UC45-X-29
30	(-0.018, -0.006)	85	2.46	UC45-X-30

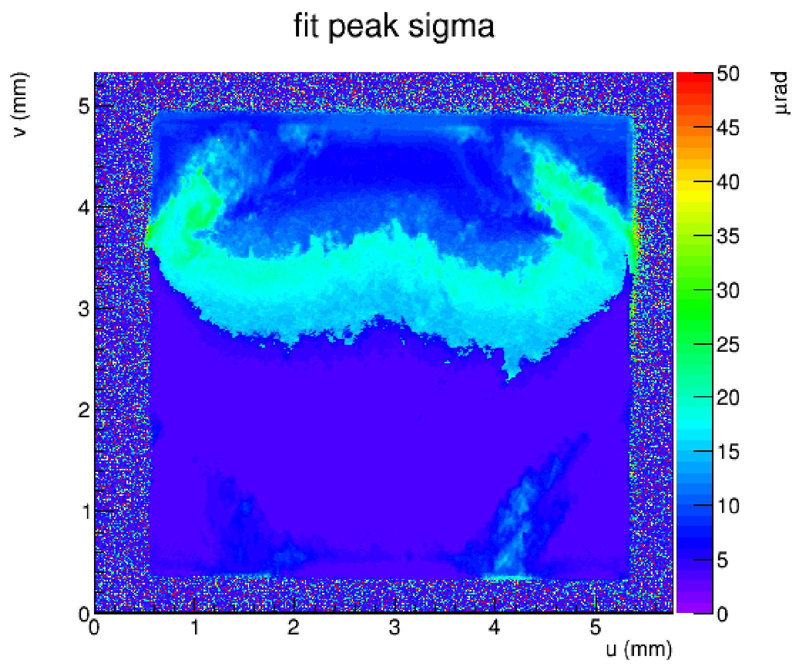

Figure: Image of rocking curve data analyzed for UC45-X_029. The bin values in the z axis are the sigma parameters of the fit made over the entire run for each individual pixel of the diamond seen by the camera.

scan number	theta range (deg)	no. steps	step size (urad)	image prefix
32†*	(-0.018, -0.006)	85	2.46	UC45-X-32

†Scan 31 was run and observed visually, but not recorded

*scan 32 was a repeat of scans 29 and 30, but the motor holding current was increased to 90%

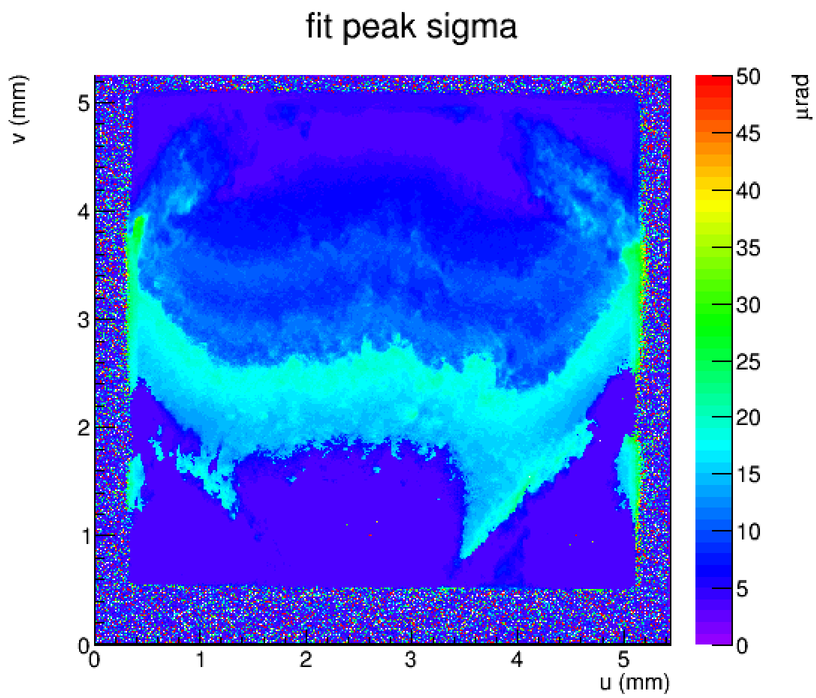

Figure: Image of rocking curve data analyzed for UC45-X_030. The bin values in the z axis are the sigma parameters of the fit made over the entire run for each individual pixel of the diamond seen by the camera.

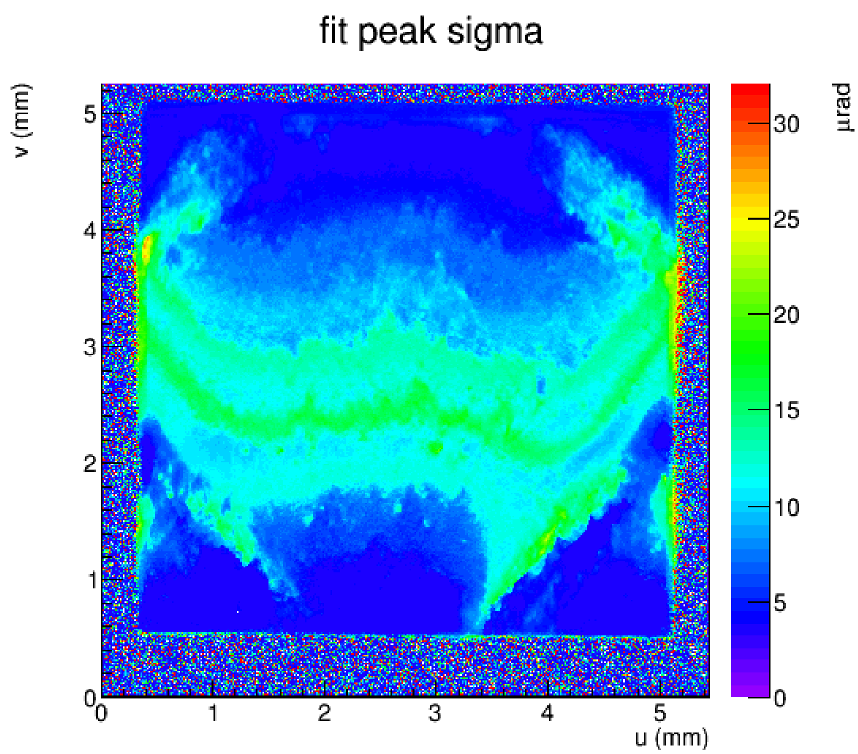

Figure: Image of rocking curve data analyzed for UC45-X_032. The bin values in the z axis are the sigma parameters of the fit made over the entire run for each individual pixel of the diamond seen by the camera.

Scan 32 was taken with the motor current increased to the maximum allowed value (dial setting 9, vs dial setting 6 that we had before). Comparing scans 30 and 32 shows that this made virtually no difference. Not sure what this is due to, but likely due to the microstepping of the motor. We returned the current to setting 6 to avoid overheating the motor.

Scans of JD70-108 in down-bounce geometry

scan number	theta range (deg)	no. steps	step size (urad)	image prefix
1*	(0.095, 0.73)	199	55.4	JD70-108-1
2	(0.595, 0.730)	191	12.3	JD70-108-2
3	(0.346, 0.546)	281	12.3	JD70-108-3
4	(0.420, 0.640)	309	12.3	JD70-108-4
5	(-0.156, 0.074)	325	12.3	JD70-108-5

*The value for the initial theta range of this scan was set too low and the data was not analyzed

After scan 2, we rotated the sample holder to place “Through on the upstream side to position 3:00 (viewed from upstream) and made a new scan, numbered 3. By mistake, we failed to set the Region of Interest in the camera for this run, so as a result we ended up with huge images of pixel dimensions 4000x2672. I had to modify the software to accommodate these images.

After scan 3, we rotated the sample holder to place “Thread” on the upstream side to position 9:00 (viewed from upstream) and made a new scan, numbered 4. This time we made sure that the camera ROI was set properly to include only the region occupied by the crystal within the camera field of view.

After scan 4, we rotated the sample holder once again to place “Thread” on the upstream side to position 12:00 and made a new scan, numbered 5. This scan was the last one in the series. As soon as it was complete, we dismounted the diamond from the mylar hoop and used conductive epoxy to fix it to the aluminum tab that will hold it in the Hall D goniometer. We then left it to cure overnight. Good day’s work!

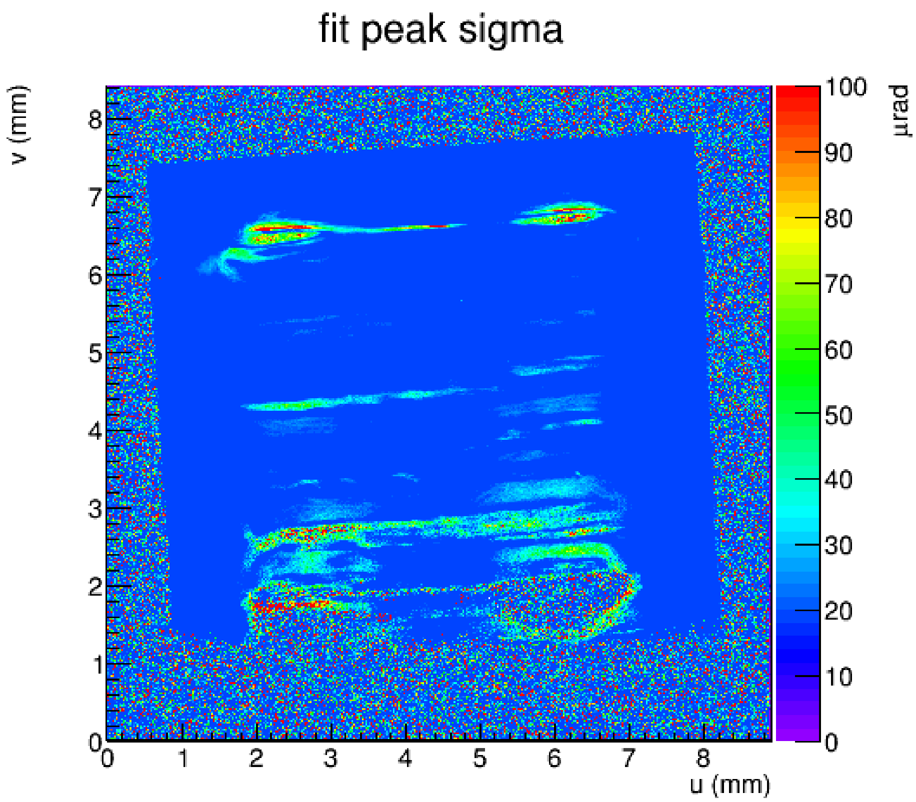

Figure: Scan 2 taken with JD70-108 mounted with “Through” on the upstream side located at 6:00 as viewed from upstream.

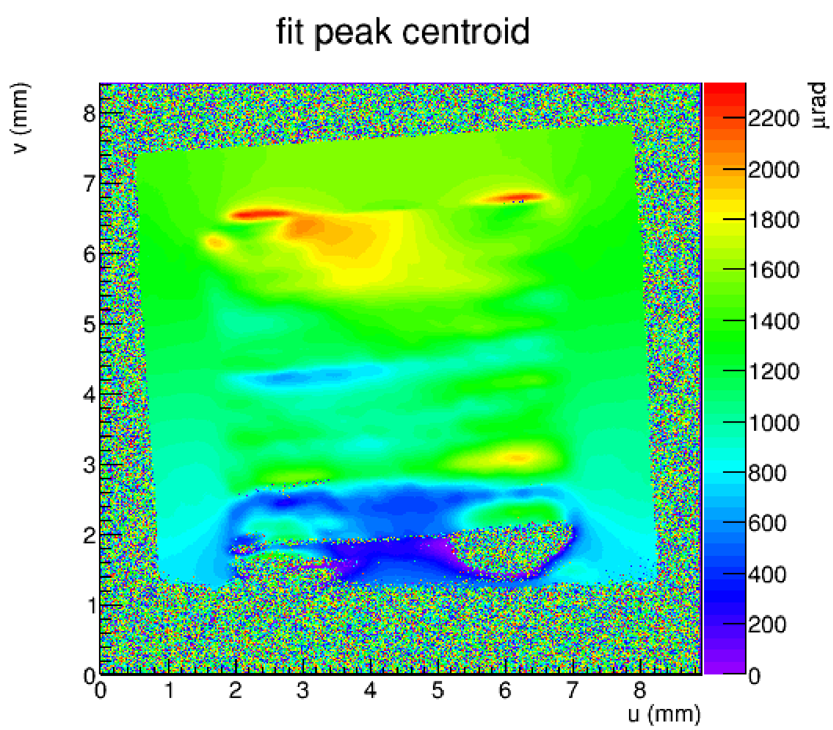

Figure: Scan 2 taken with JD70-108 mounted with “Through” on the upstream side located at 6:00 as viewed from upstream.

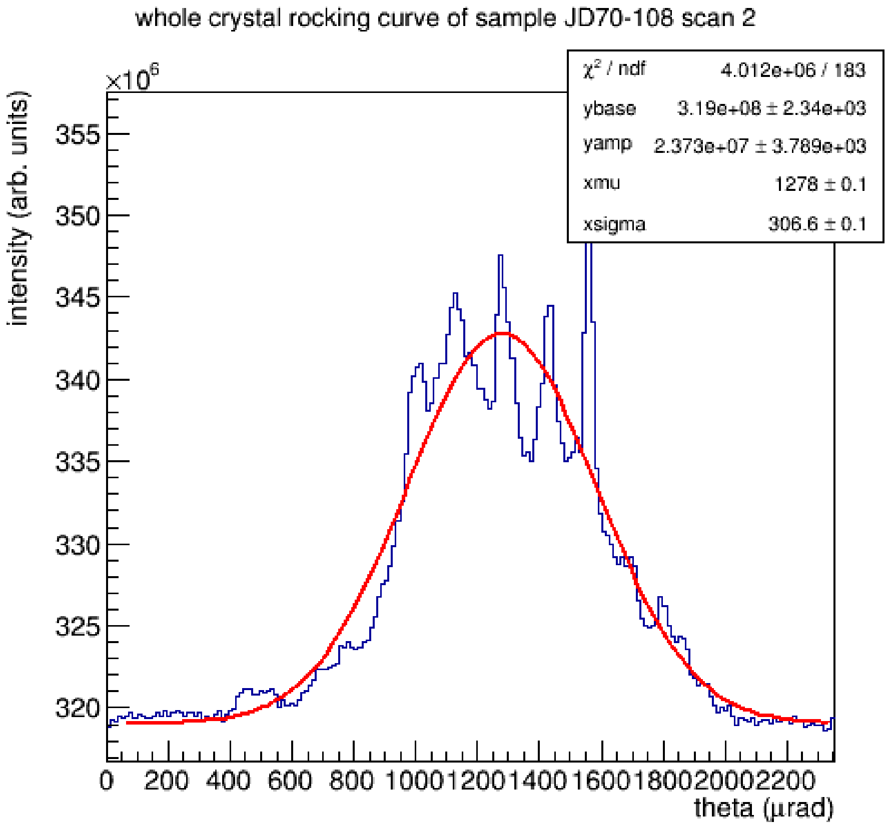

Figure: Whole crystal rocking curve, taken using scan 2

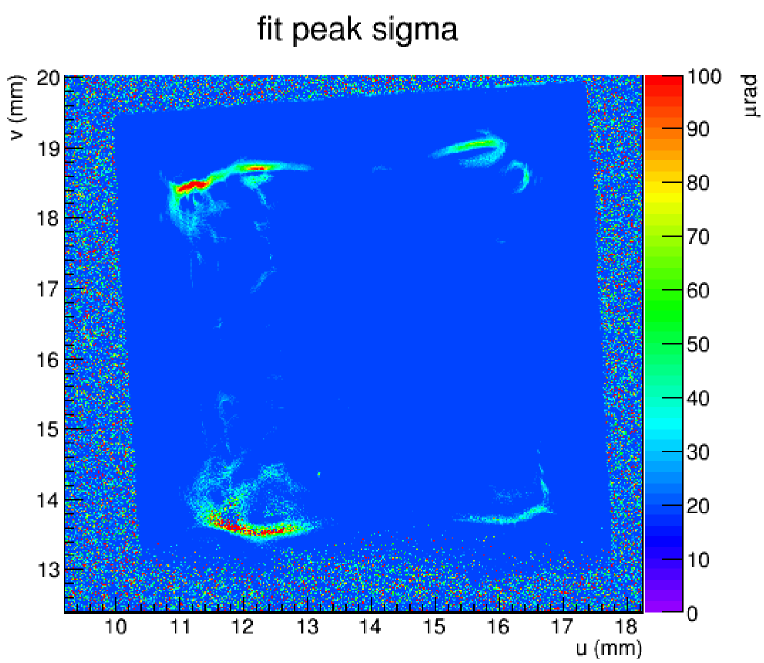

Figure: Rocking curve topograph of sigma for scan 3.

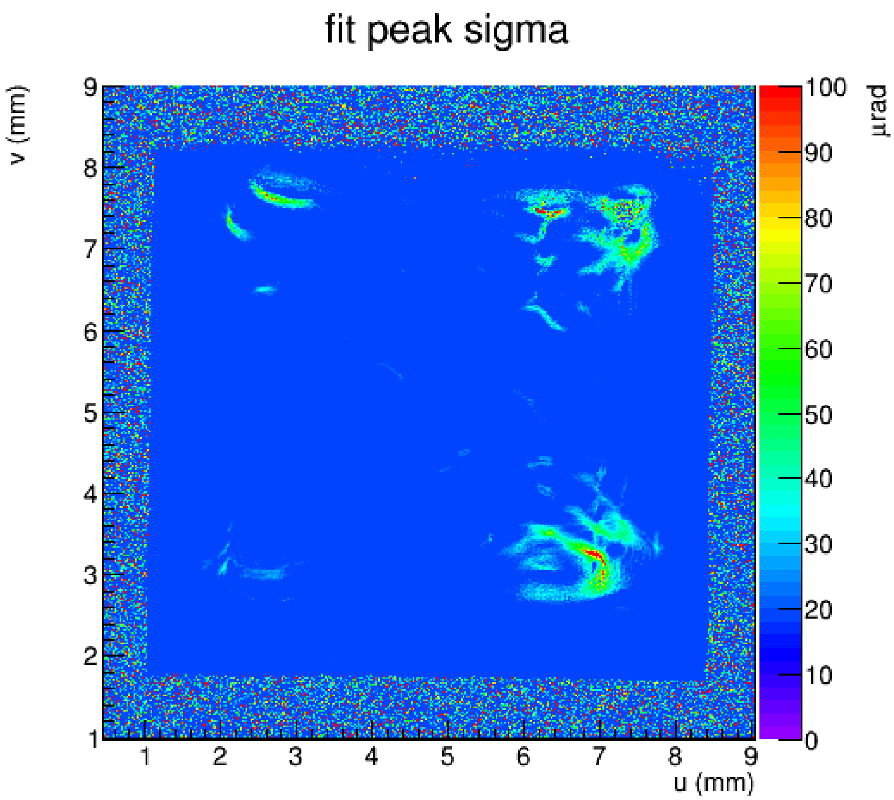

Figure: Rocking curve topograph of sigma for scan 4.

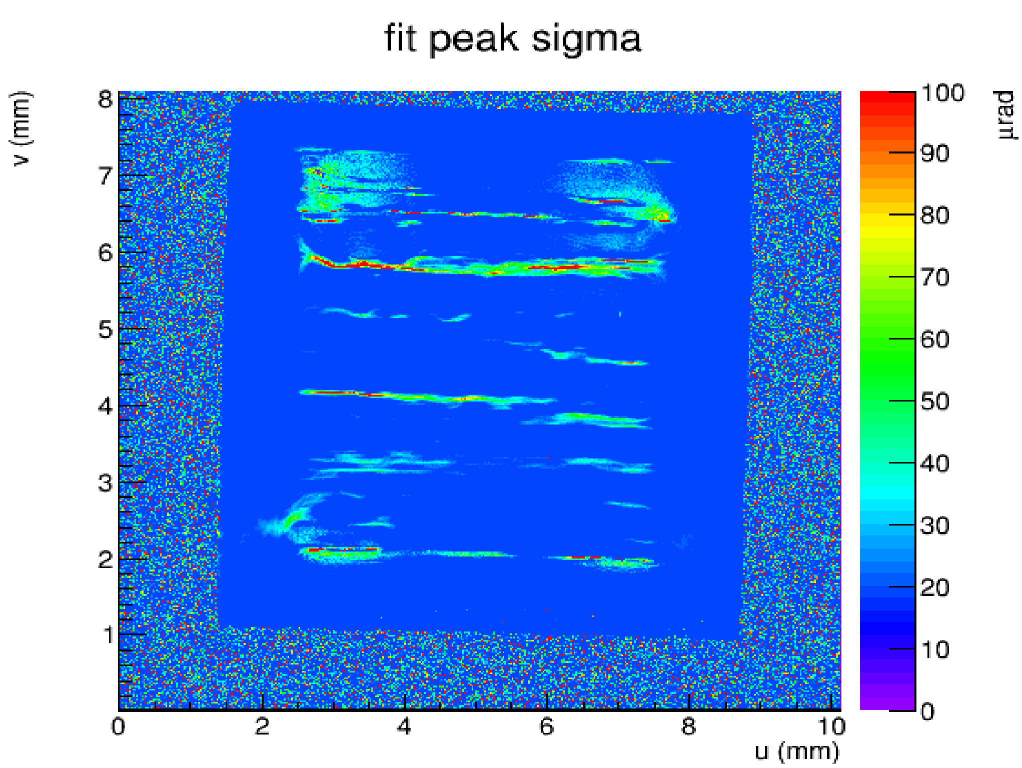

Figure: Rocking curve topograph of sigma for scan 5.

Analysis of rocking curve images

August 27, 2016 [rtj]

What can we conclude about the shape of these crystal from the rocking curves that we collected last night? Here are some questions that we need to answer regarding sample JD70-108.

1. What effects are there in these topographs coming from the beam dispersion? How can these be removed?
2. Is there residual curvature that remains in the frame? What is the shape of the frame?
3. If we place a Gaussian beam in the central region, what is the rms spread in the rocking curve centroid? How much does it vary if the spot is moved around within the central region?
4. Is there evidence of the banding structure that we saw when we studied UC45-X? What changes are present with respect to this systematic? What conclusions can be drawn from this about the root cause of these bands?

Beam dispersion

The BMIT beamline monochromator is in down-bounce geometry as shown below, so the dispersion at the target can be visualized as shown Fig. Down-Bounce above. The formula for the dispersion that relates the X-ray energy to the height above the midplane of the beam is derived from the Bragg condition for diffraction from the silicon mono crystal

$$q = 2\ k \sin\theta \qquad (1)$$

$$dk/d\theta = -q\ /\ (2 \sin\theta \tan\theta) \qquad (2)$$

For Si(2,2,0) at 20 keV mean energy of the monochromated beam, $dk/d\theta$ = 0.122 eV/urad. The distance from the source spot in the middle of the bend magnet to the sample position on our beam line is 26m. This translates into 277 urad for the full height of a 7.2 mm sample close to normal incidence, which converts to 34 eV FWHM across the full height of the sample.

Eqs. 1-2 also apply to the diamond (2,2,0) reflection, but with a different value of q = 9.820 keV instead of 6.554 keV. This energy spread translates to a diamond rocking curve angle difference of 430 urad from top to bottom. Of course this shift works together with/against the angle shift coming from the changing direction from the source to the sample as the height at the sample changes, such that the 430 urad either adds to (up-bounce) or subtracts from (down-bounce) the 277 urad. Since we are interested in minimizing this effect, we chose to do down-bounce at the sample position for the above scans 2-5, which leads to partial cancellation between the two effects. The total predicted whole-crystal rocking curve width should be 152 urad. If the crystal were perfect, the whole-crystal rocking curve FWHM would be 152 urad. This is an order of magnitude smaller than what we observed.

To take out this effect, we need to understand the sign of the dispersion correction. Take the Bragg angle θ to be a positive value and increasing as the deflection of the diffracted beam from the incident beam is increasing. The effect of beam dispersion is to contribute a positive slope to the dθ/dy relation: larger θ is required to diffract a beam with a lower k values in the top part of the beam. The effect of wavefront geometry (finite source distance) is the opposite, smaller θ at larger y. In the competition between these two, the dispersion wins out, so the net dθ/dy value is positive.

To check this against the measured figures, we need to determine whether the “Pitch motor angle corresponds to +θ or -θ, and whether the v coordinate in the figure corresponds to +y or -y. First, I look at scan UC45-X-1_001 and look at the “peak centroid” figure above. The geometry for this scan was up-bounce, so the sign of θ is such that rocking the top of the target holder upstream is a positive displacement for θ. In this configuration, both dispersion and geometry contribute positive values to the slope dθ/dy. This agrees with what is seen in the Figure “Scan 2 peak centroid” above, under the assumption that the Pitch motor advances in the direction of positive dθ(up) and the v coordinate advances along +dy. In the down-bounce configuration, the sign convention for θ flips with respect to the pitch motor, whereas the relation between y and camera image v does not change. As argued above, the dθ/dy value should be smaller but still positive in down-bounce. Therefore the sign of the slope d(Pitch motor angle) / dv should reverse and be negative in down-bounce. This is what we saw with scan UC45-X_023 and following.

Brendan observed that advancing the Pitch motor in the + direction caused the top of the target holder to move downstream, which means the + changes in the Pitch motor correspond to +dθ values in down-bounce geometry. This implies that +v in the colored topographs above also corresponds to +y in the hutch. This is different from what one sees if one views one of the camera tif files in an image viewer. I conclude from this that camera image viewer conventions take the first row of pixels to lie across the top of the viewing frame, opposite to the way that the rcpicker and makeplots visualization software works. No matter, the rcpicker/makeplots convention is what defines the v coordinate, and that corresponds to +y in the hutch, making viewing these images very simple to interpret.

To remove beam dispersion effects from the down-bounce topographs, just add a linear function to the peak centroid image, as illustrated in Eq. 3.

$$\theta(v) \mathrel{+}= v * 21 \text{ urad/mm} \qquad (3)$$

This is a small correction when compared to the whole-crystal rocking curve width near 1500 urad that was observed for JD70-108, so none of the conclusions we draw from those data are sensitive to the details of the beam dispersion.

Frame curvature of JD70-108

To discern the sense of curvature from these data, we need to know how the diamond was held in the mylar hoop. Here is a picture to help visualize the setup for scan JD70-108_002.

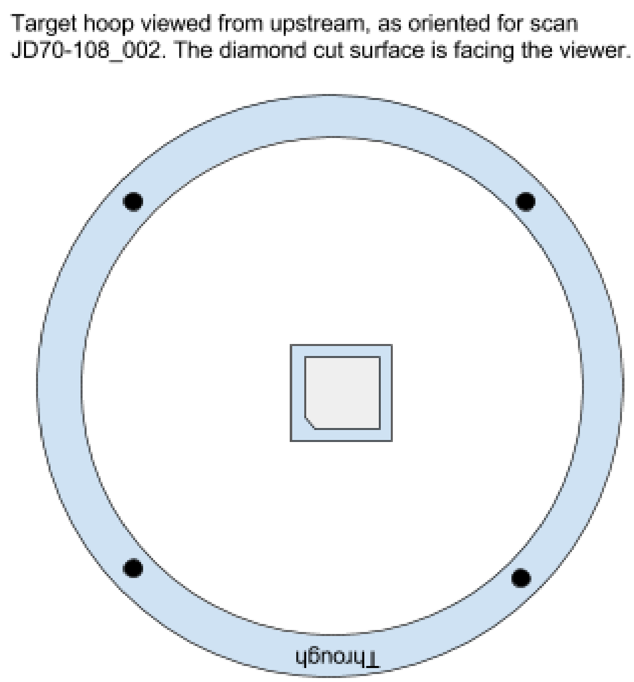

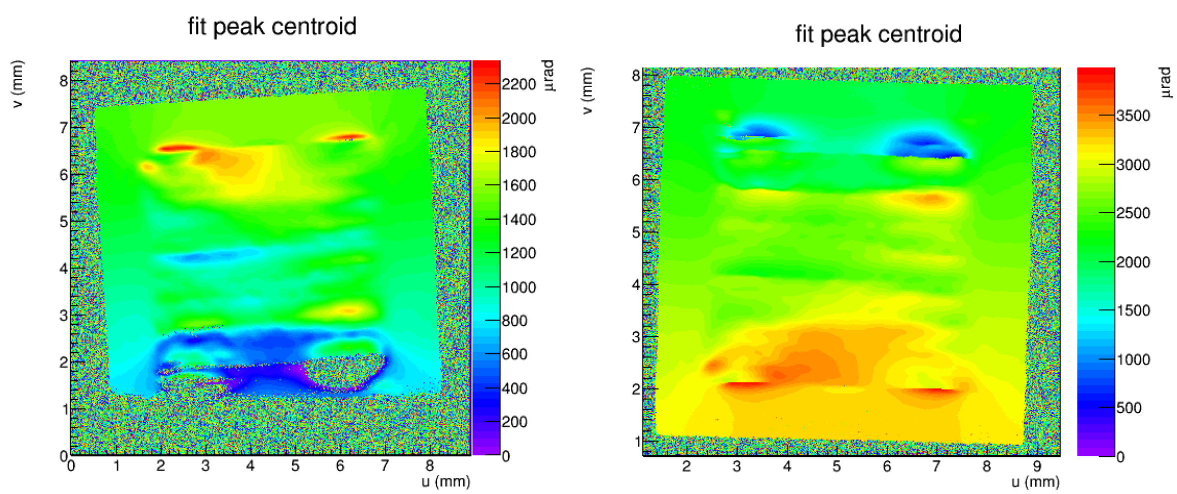

Figure: Rocking curve peak centroids from scan JD70-108_002 (left) and JD70-108_005 (right) viewed side-by-side, so one can read off the curvature of the cyrstal along the vertical direction in this view.

From the above side-by-side comparison, the full width of the whole-crystal rocking curves are:

scan 2 1750 - 750 = 1000 urad ± 100 urad
scan 5 3200 - 1800 = 1400 urad ± 100 urad

The difference between these two should be 2 * 150 = 300 urad (from beam dispersion, see previous section) which is in agreement with the above measurements within errors. The average value of 1200 ± 100 urad is the result after the effects of dispersion are removed. The resulting radius of curvature of the crystal along this axis comes out to be

R(1,5) = 7.2mm / 1200urad = 6.0 m

Curvature measured by laser spot divergence

To see if we could measure this value using surface reflection from the surface, we set up a green laser facing the back (polished) side of the diamond. The distance from the source to the diamond was 220 cm. We then measured the spot size as a function of distance from the diamond and used these values to determine the post-reflection divergence angle. Comparison of the divergence angle from the diamond reflection with that from a glass slide (assumed to be flat) can be interpreted to give the curvature of the diamond.

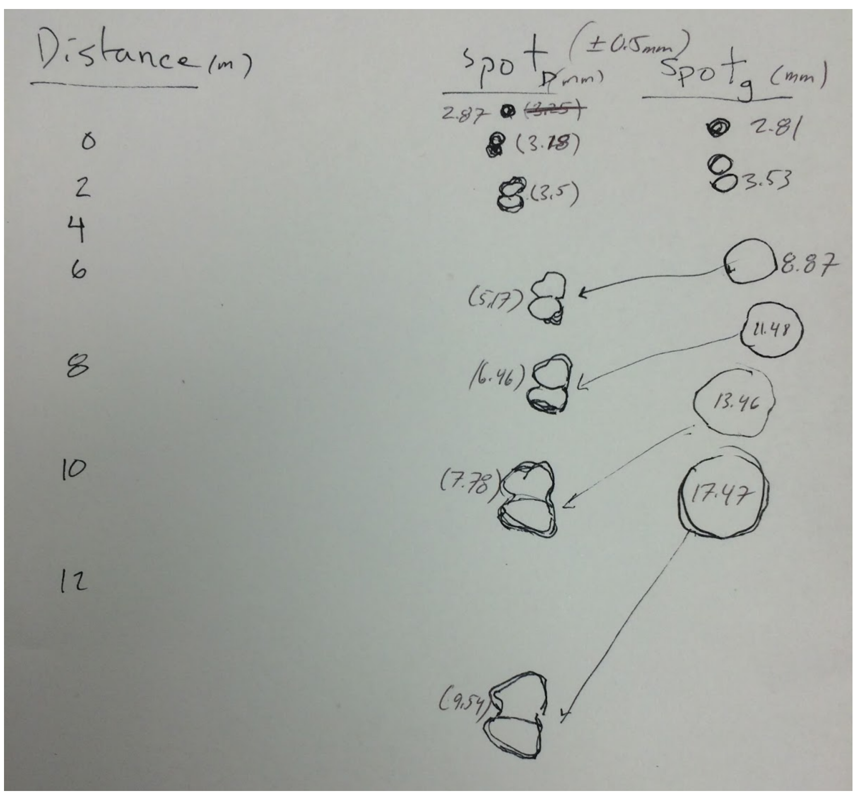

Figure: Emittance measurement data taken using 4.9mW green laser incident the backside of JD70-108 and the glass reference slif on the diamond goniometer mount. The outlines in the “spot” columns are the area of the spot at the corresponding distance away from the diamond/glass.

analysis of laser spot divergence data

August 29, 2016 [rtj]

The crude measurements shown on the above sheet of paper should be sufficient to get an initial estimate for the curvature of the back side of JD70-108. The values Brendan extracted from the hand-drawn contours are given in the table below, and plotted in the following figure.

Table: Meaasured spot diameters taken varying distances from the reflection surface. The cell highlighted in yellow was inserted artificially by visual interpolation between surrounding points because it seems that Brendan skipped this D value when he was measuring the spot sizes for the glass (see sheet above).

meas. error	0.0005	m	
distance (m)	JD70-108-V (m)	JD70-108-H (m)	glass (m)
0	0.00287	0.00287	0.00281
2	0.00318	0.00318	0.00353
4	0.00350	0.00537	0.006
6	0.00517	0.00731	0.00887
8	0.00646	0.01	0.01148
10	0.00778	0.01254	0.01346
12	0.00954	0.015	0.01747

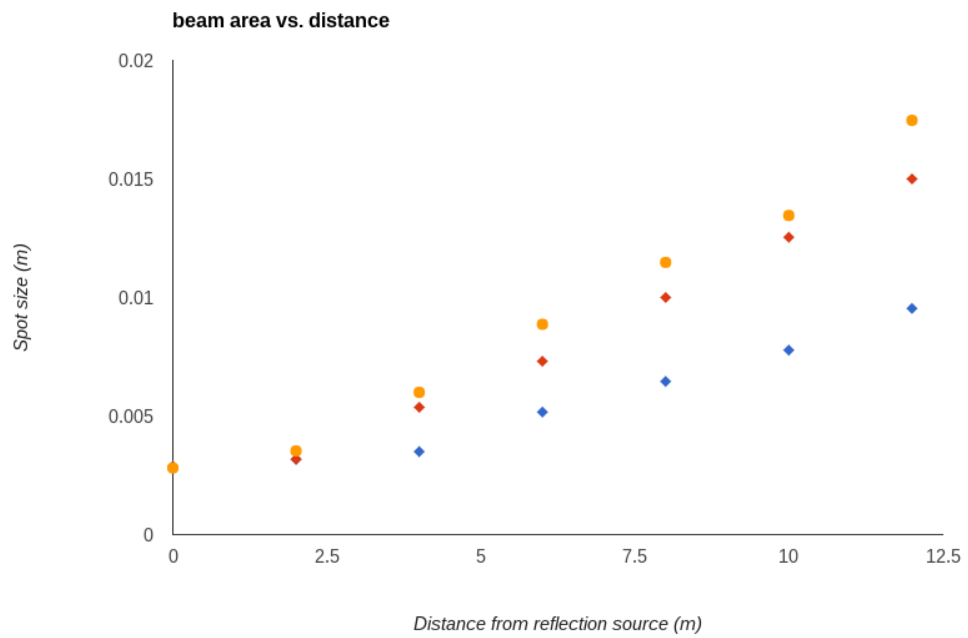

Figure: Reflected spot diameter from a 5W laser from the back side of JD70-108 (blue points vertical axis, red points horizontal) compared with a planar glass side (yellow points).

The following simple model was used to fit these data and estimate the horizontal and vertical radii of curvature of the diamond, assuming that the glass slide is planar.

- Assume that the laser has a waist position at (or near) its location. Call the distance from the waist to the reflection surface D_0.
- At the waist, the position x_0 and direction α_0 random variables of rays are described by independent Gaussian distributions with variances $V(x_0)$ and $V(\alpha_0)$ where x_0, α_0 are transverse displacement and angle from the beam axis, respectively, at the waist.
- After reflection, the displacement x_1 is the value of x at the reflection surface, and the ray angle becomes α_1 which is given in the parabolic reflector approximation by Eq. 2.1.

$$\alpha_1 = \alpha_0 - 2\, x_1 / R \tag{2.1}$$
$$x_1 = x_0 + \alpha_0\, D_0 \tag{2.2}$$

where R is the radius of curvature of the mirror. Linear propagation gives the transverse displacement $x(D)$ for the ray that starts off at the waist with coordinates (x_0, α_0), where D is the distance from the mirror after reflection.

$$\begin{aligned} x(D) &= x_1 + \alpha_1\, D \\ &= x_0\,(1 - 2\, D / R) + \alpha_0\,(D + D_0\,(1 - 2\, D / R)) \end{aligned} \tag{2.3}$$

From the independence of random variables x_0 and α_0 it follows that the spot size $V(D)$ at any distance D from the mirror is given by Eq. 2.4.

$$V(D) = V(x_0)\,(1 - 2\, D / R)^2 + V(\alpha_0)\,(D + D_0\,(1 - 2\, D / R))^2 \tag{2.4}$$

Eq. 2.4 is a quadratic function of D as $V(D) = A + B\,D + C\,D^2$ where

$$A = V(x_0) + V(\alpha_0)\, D_0^2$$
$$B = 2\, D_0\, V(\alpha_0)\,(1 - 2\, D_0 / R) - 4\, V(x_0) / R$$
$$C = 4\, V(x_0) / R^2 + V(\alpha_0)\,((1 - 2\, D_0 / R)^2$$

As R goes to infinity, $A \rightarrow V(x_0) + V(\alpha_0)\, D_0^2$, $B \rightarrow 0$, $C \rightarrow V(\alpha_0)$ as expected. I carried out a unified least-squares fit to the data listed above using this model. where the constants $V(x_0)$, $V(\alpha_0)$, D_0, and R were allowed to vary freely. The results are shown below, with the error bars estimated based on how far the parameter could be varied without increasing the chi-square by more than 1. The measurement errors for all points were taken to be equal.

horizontal:	$R = 4.3 \pm 0.8$ m
vertical:	$R = 19.8 \pm 4.2$ m
unified:	$D_0 = 1.34 \pm 0.15$ m
unified:	$V(x_0) = 1.37 \pm 0.20$ mm
unified:	$V(\alpha_0) = 1.23 \pm 0.03$ mrad

Scans of JD70-108 in epoxy mount

August 27, 2016 [BJP]

Scan JD70-108-6 was started with the dog ear of the diamond in the left corner as viewed from upstream with the diamond cut surface facing the viewer (see image below).

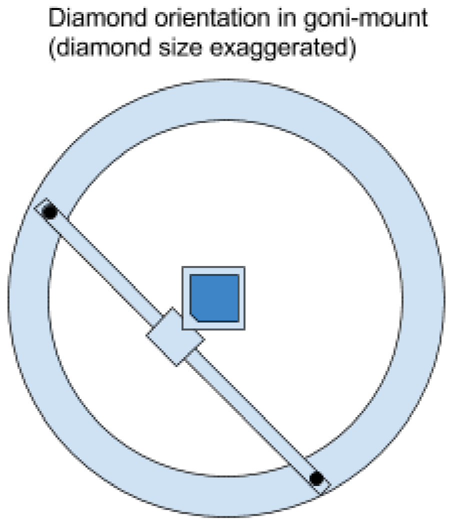

Figure: Illustration of the orientation of the diamond for scan JD70-108-[6,7,8] in the goni-mount as viewed from upstream. The cut surface is facing the viewer.

This was the first scan made after the diamond was glued to the aluminum tab and was secured to the goniometer mount. Scan JD70-108-8 is a repeat of JD70-108-6.

scan number	theta range (deg)	no. steps	step size (urad)	image prefix
6	(-0.62, -0.51)	155	12.3	JD70-108-6
7*	(-1.08,-0.89)	268	12.3	JD70-108-7
8**	(-1.08,-0.89)	268	12.3	JD70-108-8

*scan 7 was performed without the shutter opened and so it was not pushed to disk.
August 28, 2016 [bjp]
**we must have been tired when we were rotating the diamond, we moved the ring and repositioned the bar that the diamond is bolted to in such a way that it was in the same orientation as JD70-108-6.

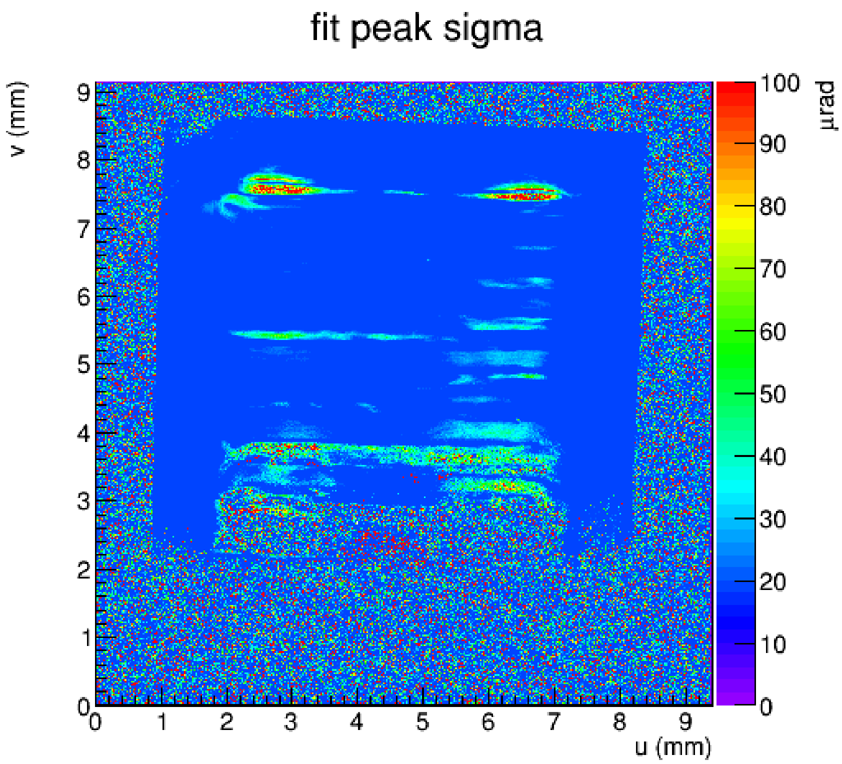

Figure: Rocking curve topograph of sigma for scan 6

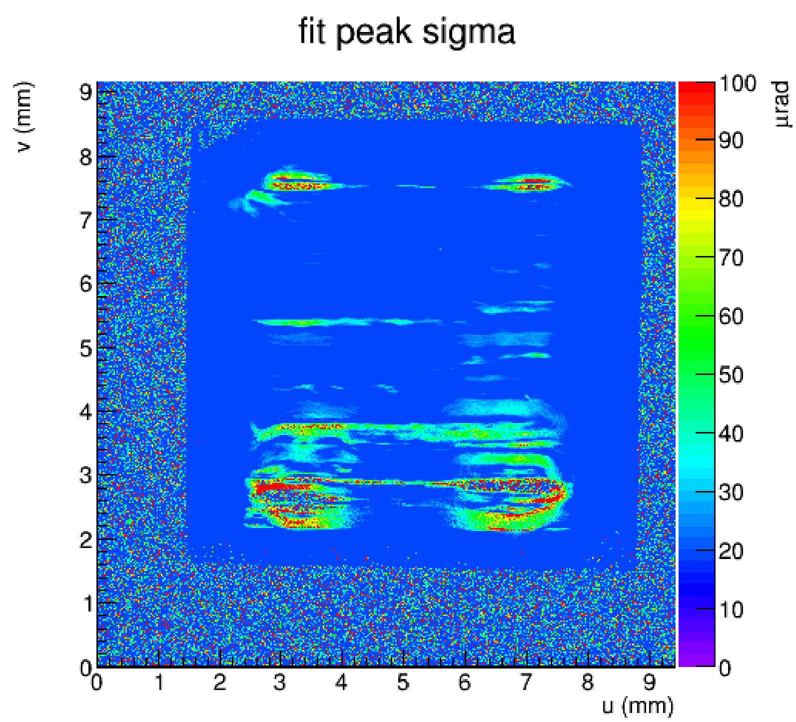

Figure: Rocking curve topograph of sigma for scan 8

The first thing on the list today is finishing the scans of JD70-108 by taking scans in the other three orientations. I just looked at the beam current monitor and there was an apparent trip. Seems that beam won't likely be back before noon.

The diamond is now rotated 90° to the following orientation as viewed from upstream.

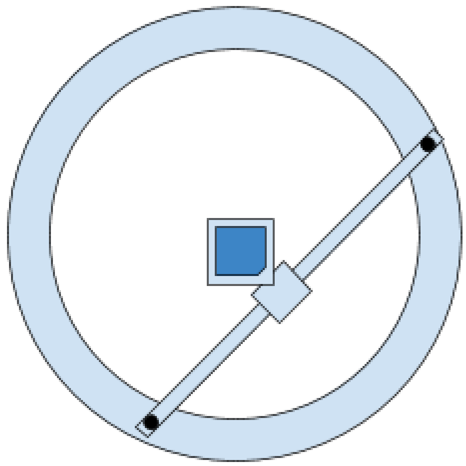

Figure: Illustration of the orientation of the diamond for scan JD70-108-9 in the goni-mount.

scan number	theta range (deg)	no. steps	step size (urad)	image prefix
9	(-0.8, -0.62)	254	12.3	JD70-108-9
10	(-0.8,-0.59)	296	12.3	JD70-108-10
11	(0.48, 0.7)	310	12.3	JD70-108-11

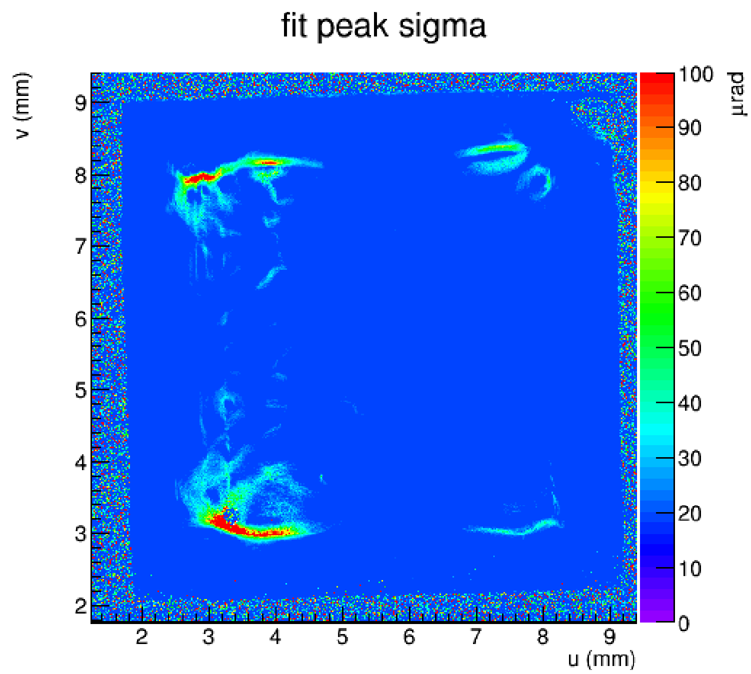

Figure: Rocking curve topograph of sigma for scan 9

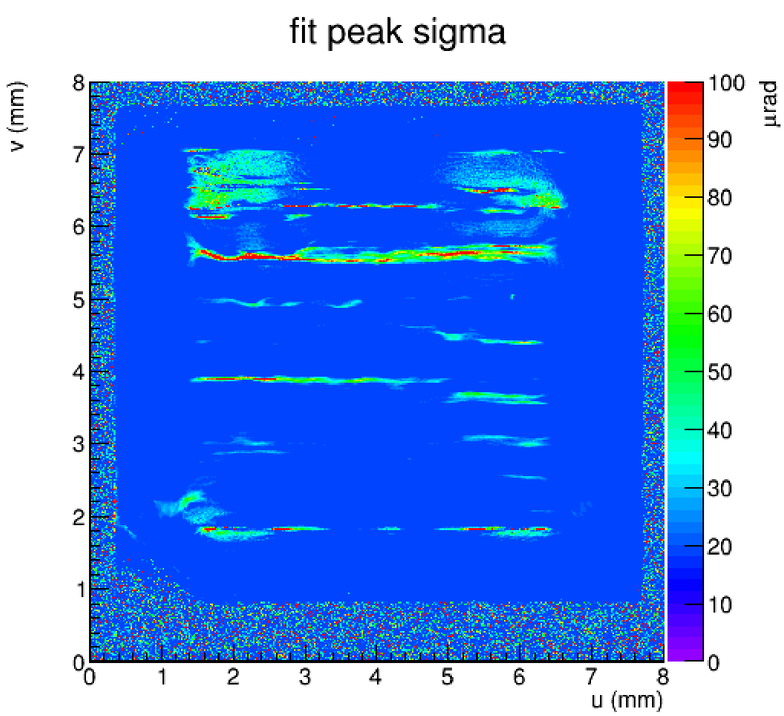

Figure: Rocking curve topograph of sigma for scan 10

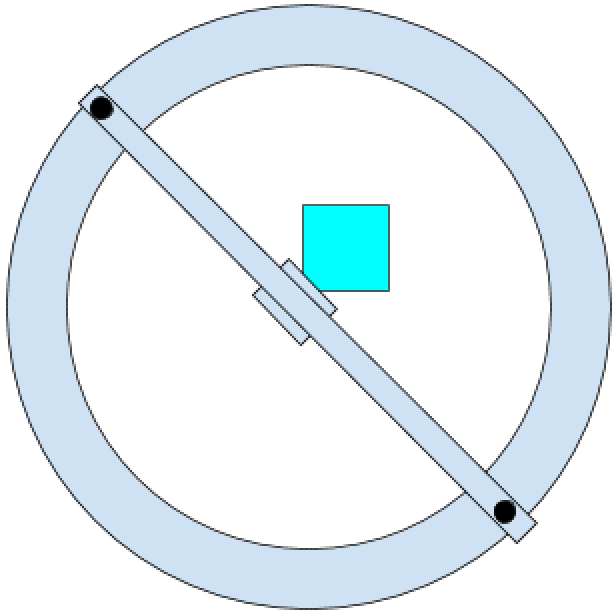

Figure: Diamond orientation for scan JD70-108-10

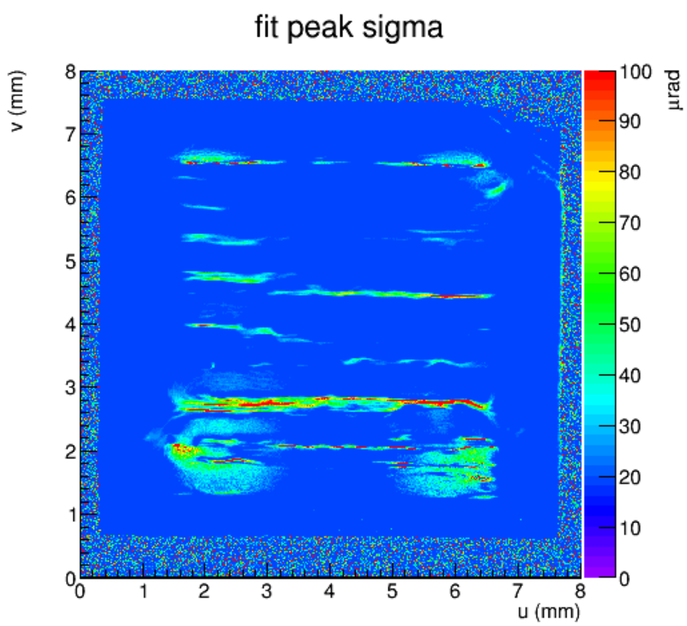

Figure: Rocking curve topograph of sigma for scan 11

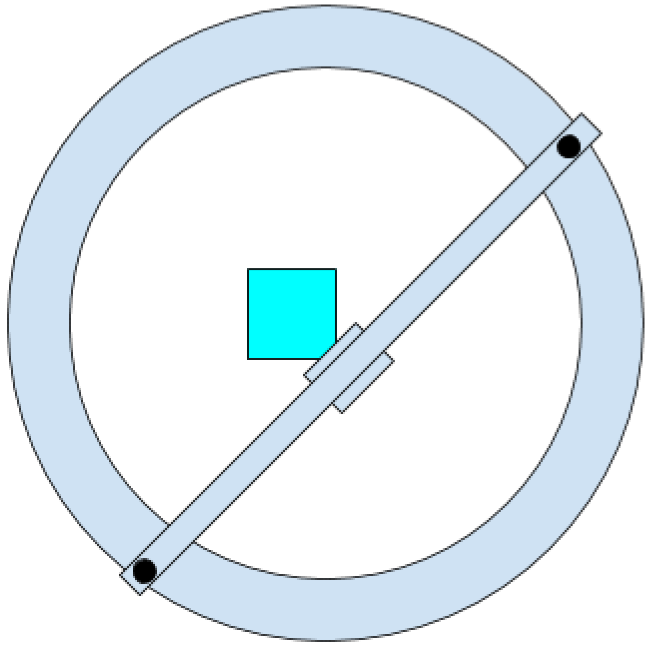

Figure: Diamond orientation for scan JD70-108-11

Scans 9,10,11 are finished. Now I will measure the rocking curve of a pristine 7mmx7mm crystal mounted in the mylar hoop once more.

Scans of JD70-101 in down-bounce geometry

JD70-101 is a pristine 7mm sample that we will use to calibrate the oscillations in the rocking curve measurements, believed to be a result of non-linearity in the theta motor. I have oriented the diamond in the mylar hoop so that the first rocking curve measurement will have “Through” at the 12:00 position when viewed from upstream. As expected, this crystal has a very narrow rocking curve. I will use the 0.0001412 degree resolution as before with UC45-X.
I will take 4 scans of each orientation so that we can compare the positions of the oscillations (if present).

scan number	theta range (deg)	no. steps	step size (urad)	image prefix
1	(-0.593,-0.577)	112	2.46	JD70-101-1
2	(-0.593,-0.577)	112	2.46	JD70-101-2
3	(-0.593,-0.577)	112	2.46	JD70-101-3
4	(-0.593,-0.577)	112	2.46	JD70-101-4

JD70-101 has been rotated 90° so that the “Through” logo is now in the 3:00 position as viewed from upstream.

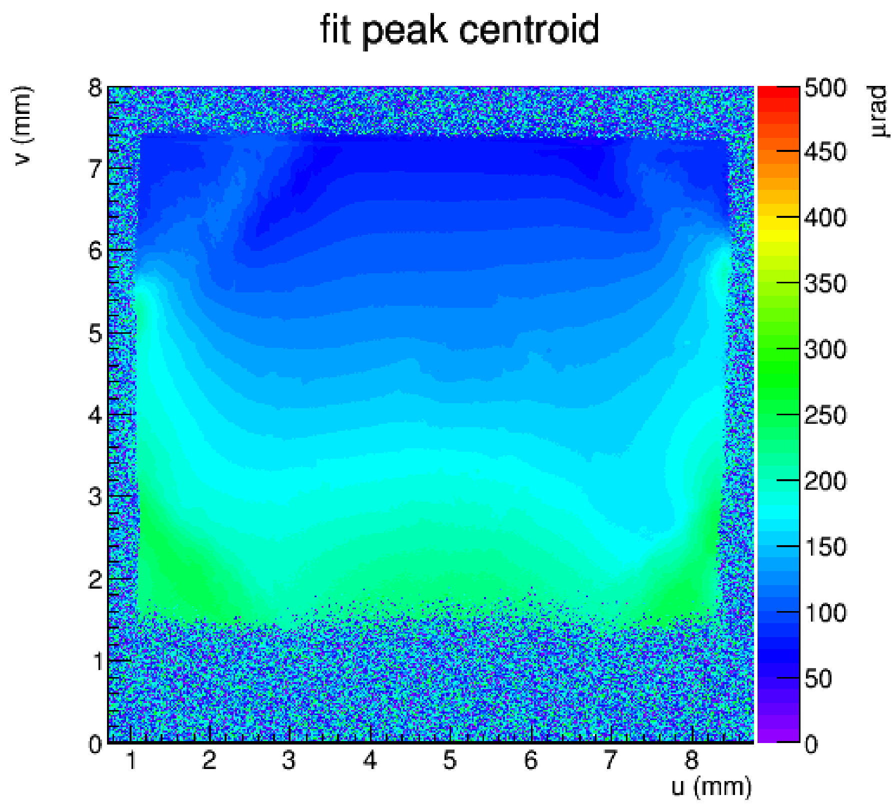

Figure: Rocking curve topograph of mu for scan 1

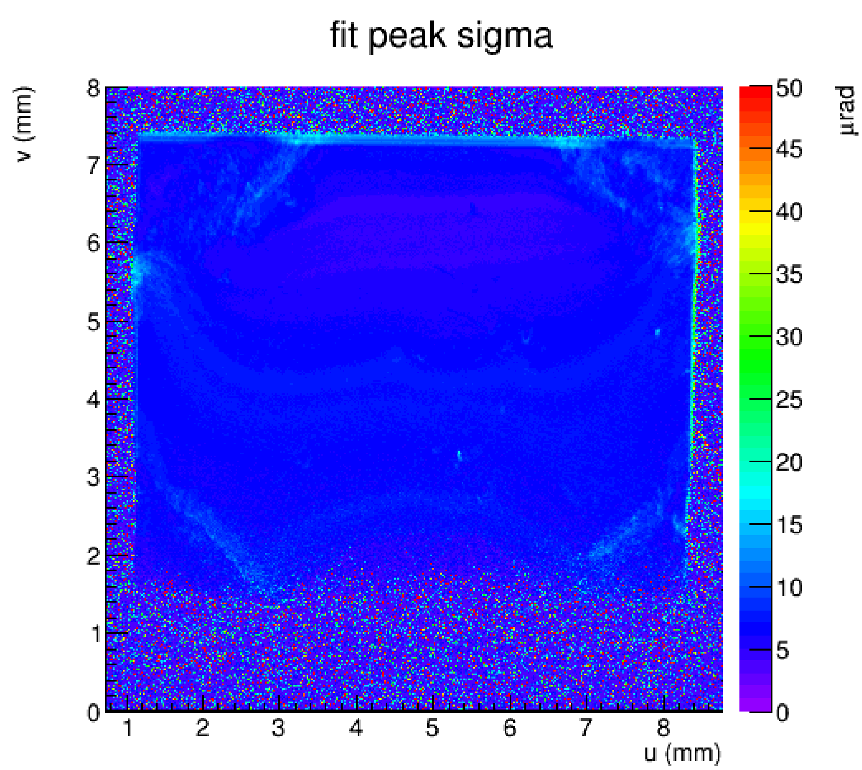

Figure: Rocking curve topograph of sigma for scan 1

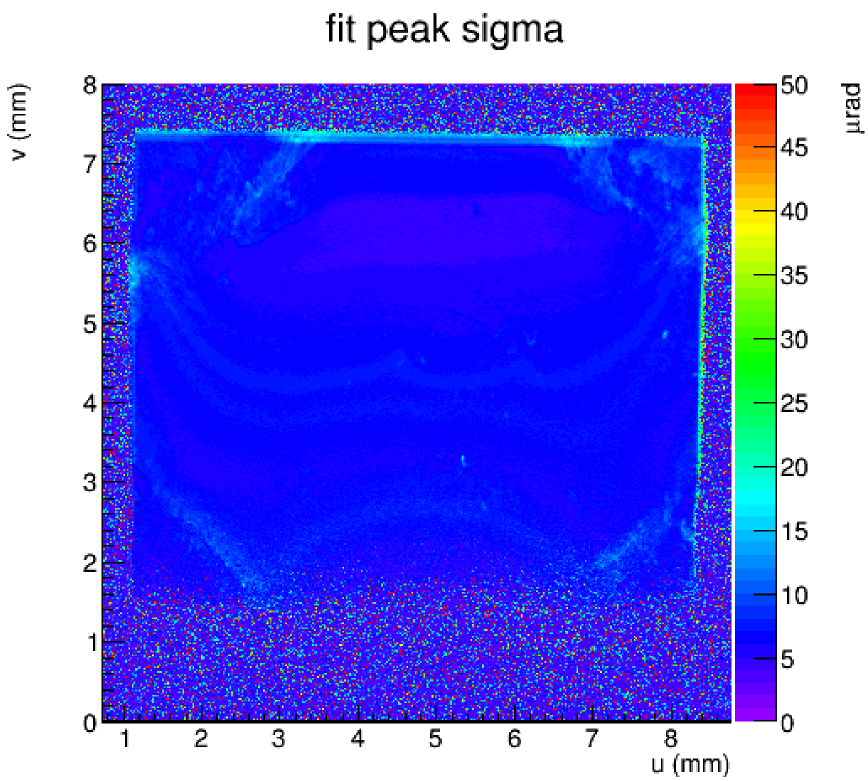

Figure: Rocking curve topograph of sigma for scan 2

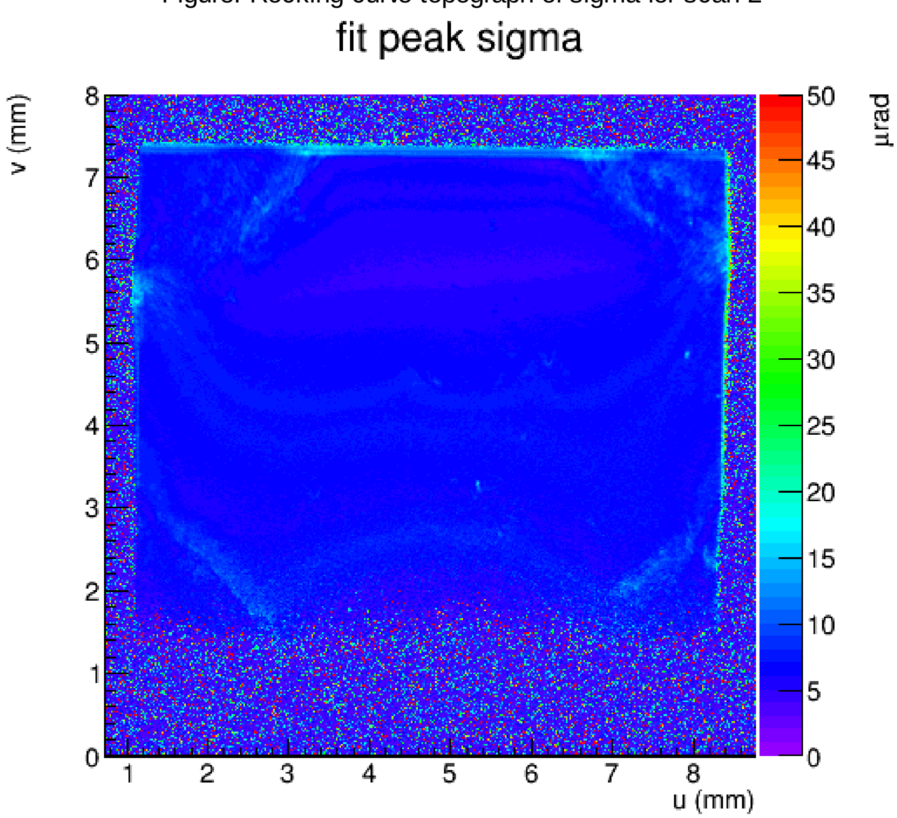

Figure: Rocking curve topograph of sigma for scan 3

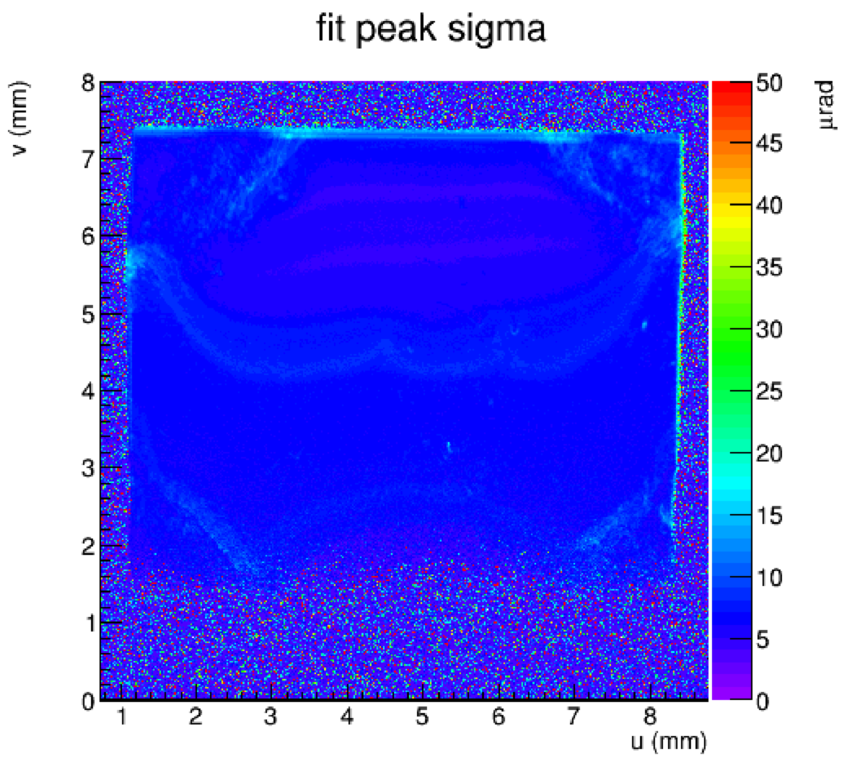

Figure: Rocking curve topograph of sigma for scan 4

scan number	theta range (deg)	no. steps	step size (urad)	image prefix
5	(0.235, 0.252)	119	2.46	JD70-101-5
6	(0.235, 0.252)	119	2.46	JD70-101-6
7	(0.235, 0.252)	119	2.46	JD70-101-7
8	(0.235, 0.252)	119	2.46	JD70-101-8

The diamond was rotated 180° in phi so that the “Through” logo is now facing the opposite direction at the 3:00 position if viewed from DOWNSTREAM

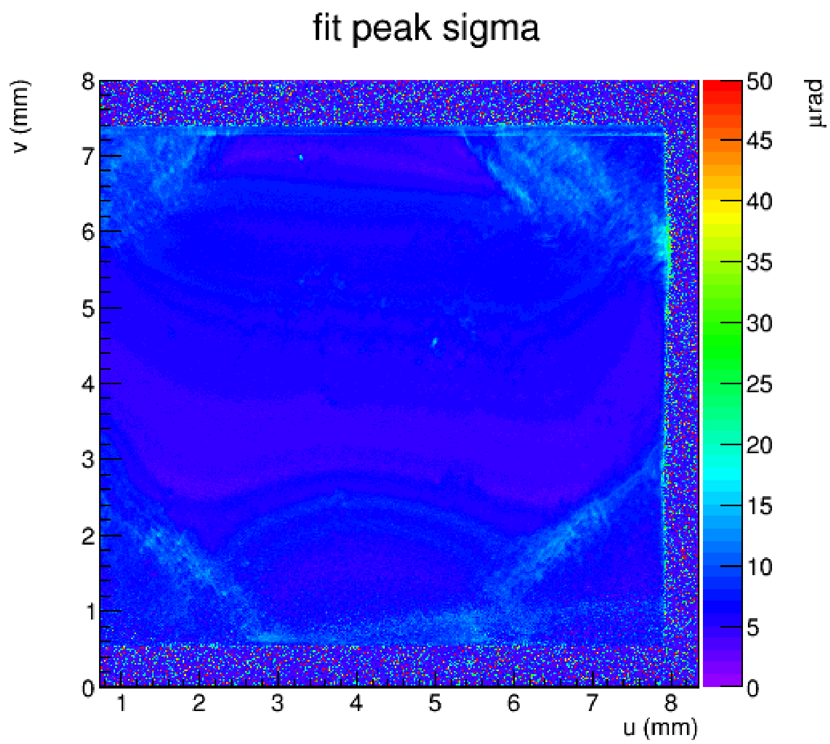

Figure: Rocking curve topograph of sigma for scanc 5

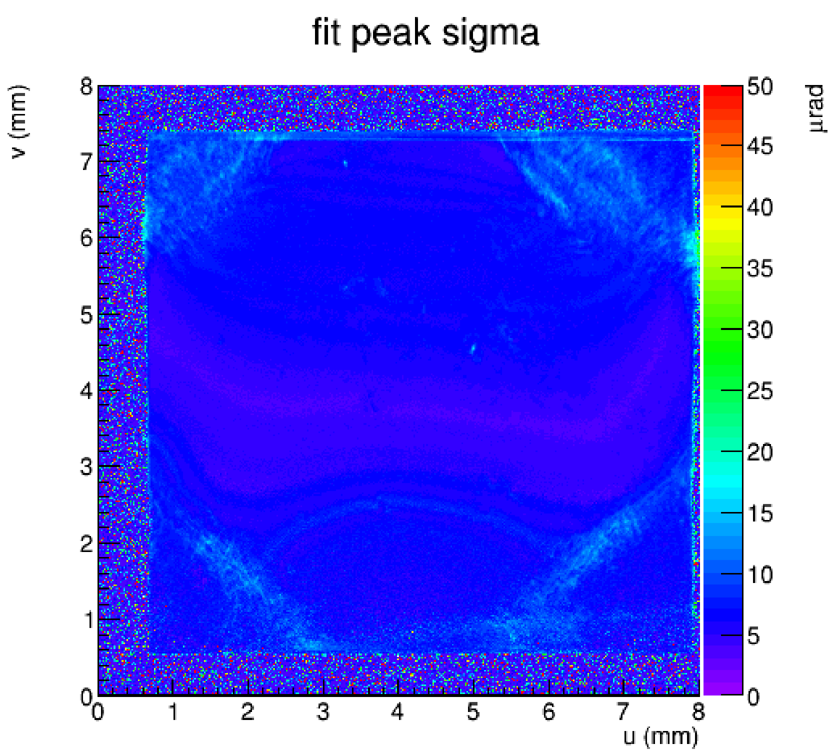

Figure: Rocking curve topograph of sigma for scan 6

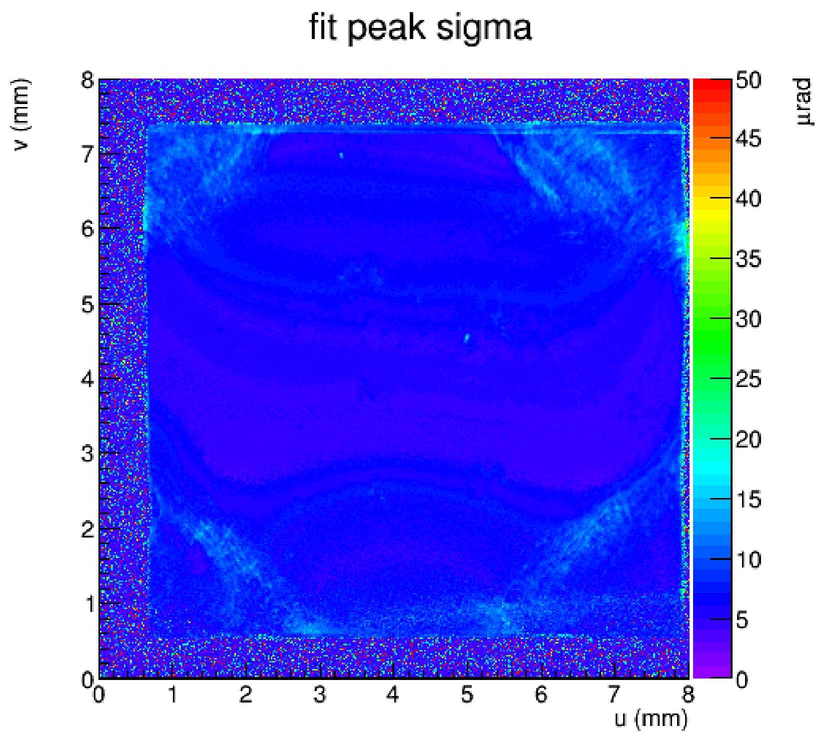

Figure: Rocking curve topograph of sigma for scan 7

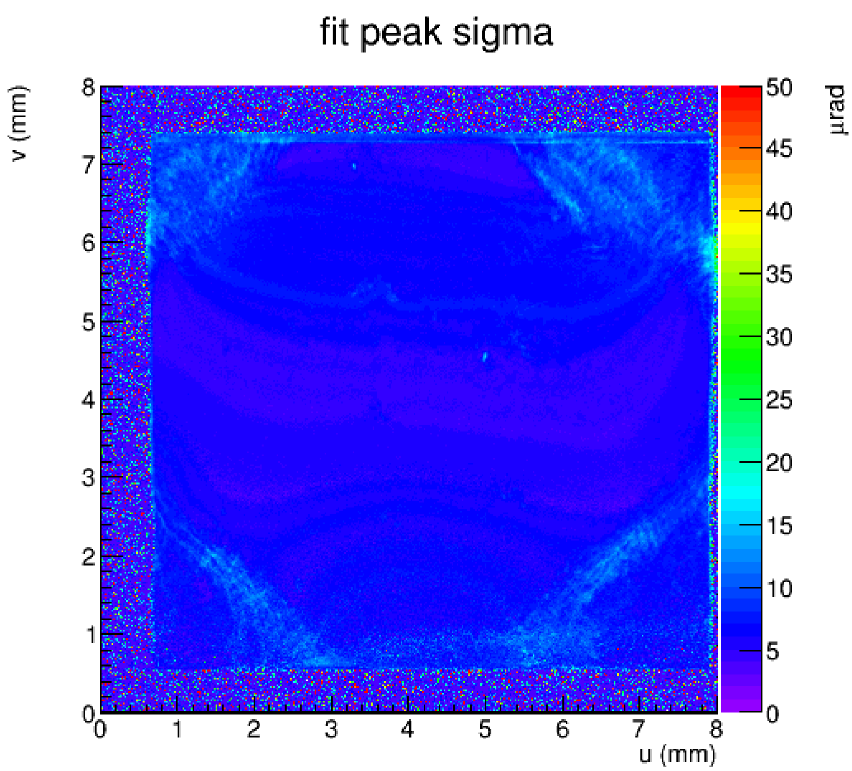

Figure: Rocking curve topograph of sigma for scan 8

scan number	theta range (deg)	no. steps	step size (urad)	image prefix
9	(-0.185.,-0.171)	98	2.46	JD70-101-9
10	(-0.185.,-0.171)	98	2.46	JD70-101-10
11	(-0.185.,-0.171)	98	2.46	JD70-101-11
12	(-0.185.,-0.171)	98	2.46	JD70-101-12

The crystal was rotated for the fourth and final time so that the “Through” logo was facing the 12:00 position if viewed from downstream.

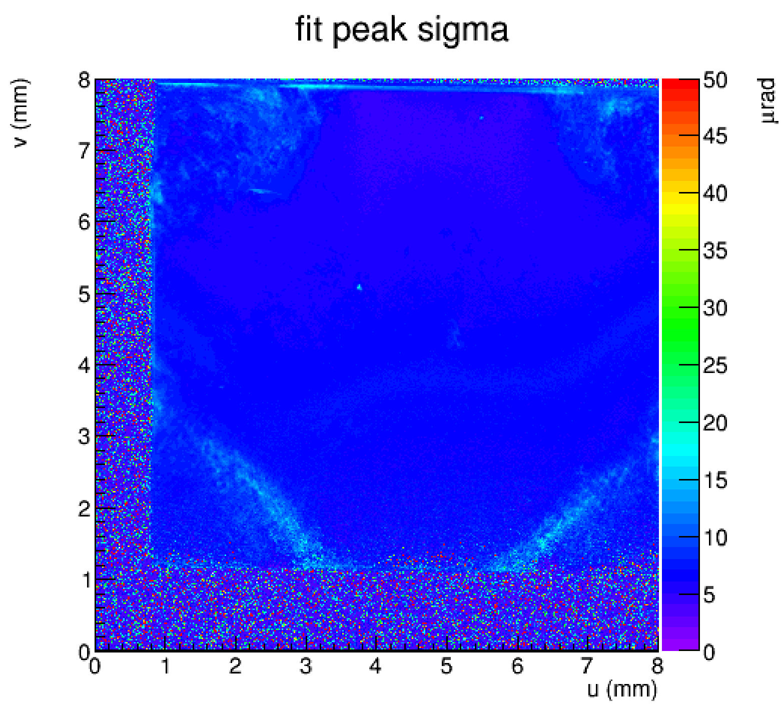

Figure: Rocking curve topograph of sigma for scan 9

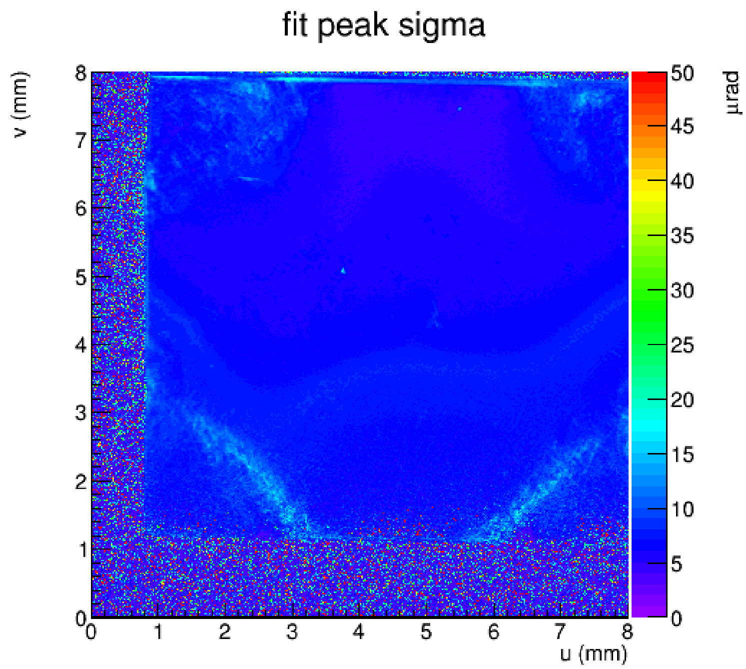

Figure: Rocking curve topograph of sigma for scan 10

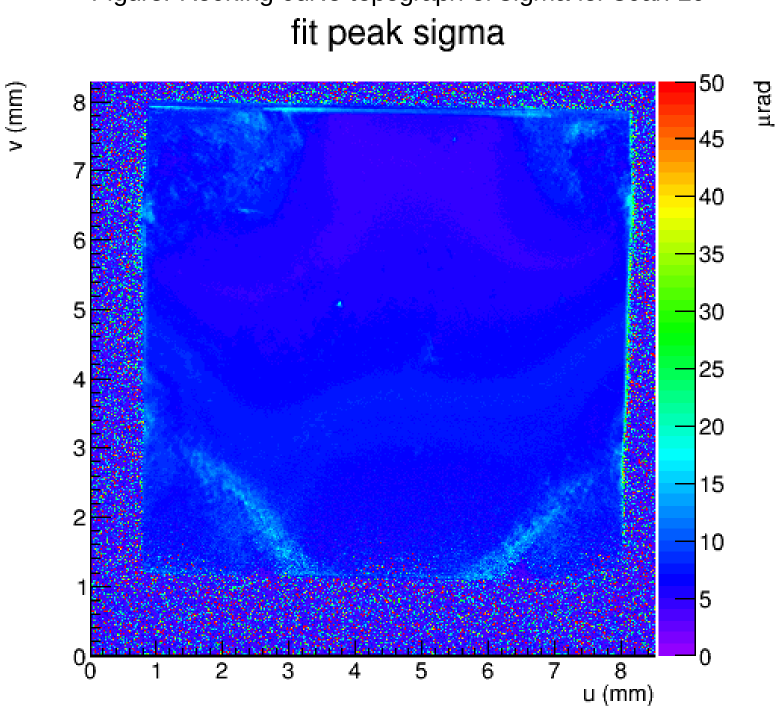

Figure: Rocking curve topograph of sigma for scan 11

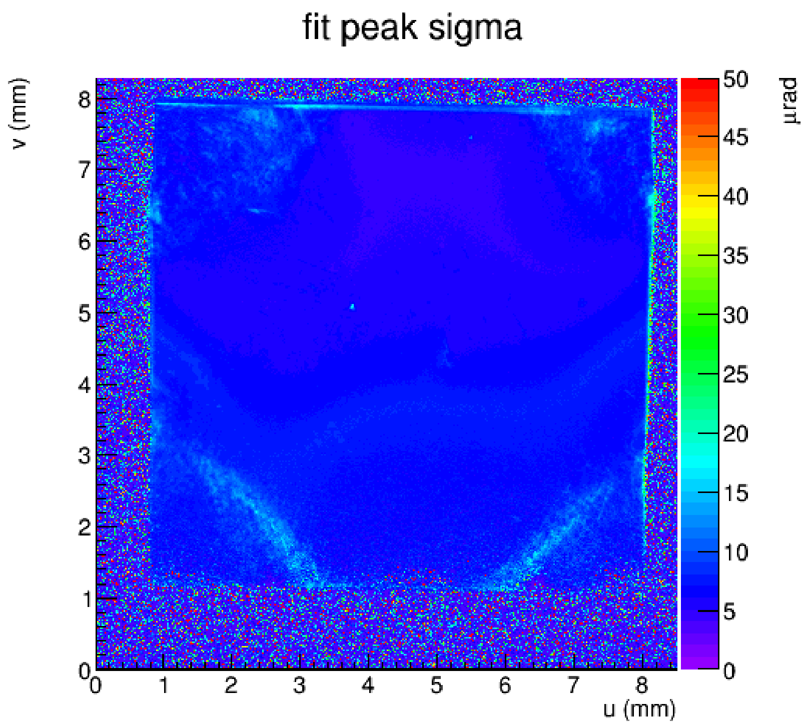

Figure: Rocking curve topograph of sigma for scan 12

scan number	theta range (deg)	no. steps	step size (urad)	image prefix
13	(0.615, 0.628)	91	2.46	JD70-101-9
14	(0.615, 0.628)	91	2.46	JD70-101-10
15	(0.615, 0.628)	91	2.46	JD70-101-11
16	(0.615, 0.628)	91	2.46	JD70-101-12

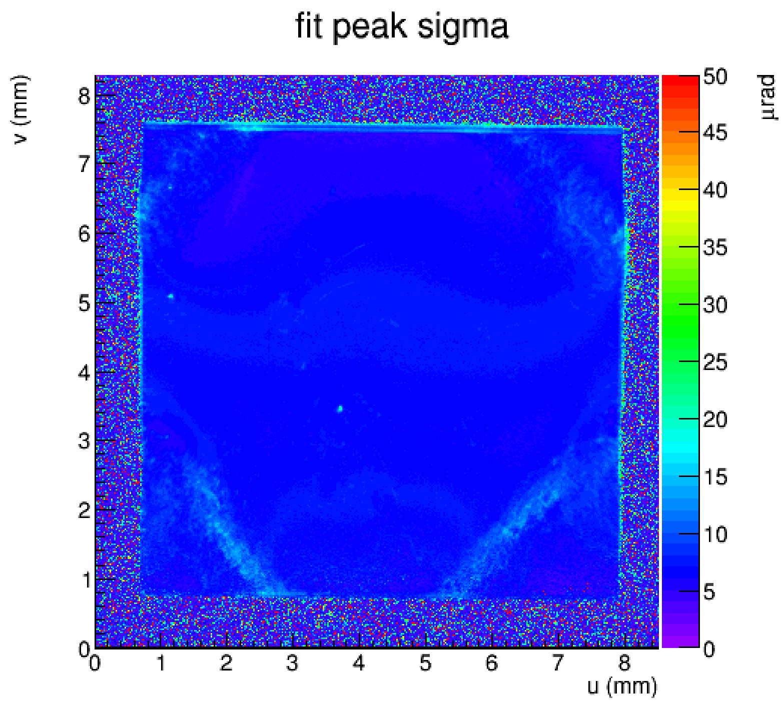

Figure: Rocking curve topograph of sigma for scan 13

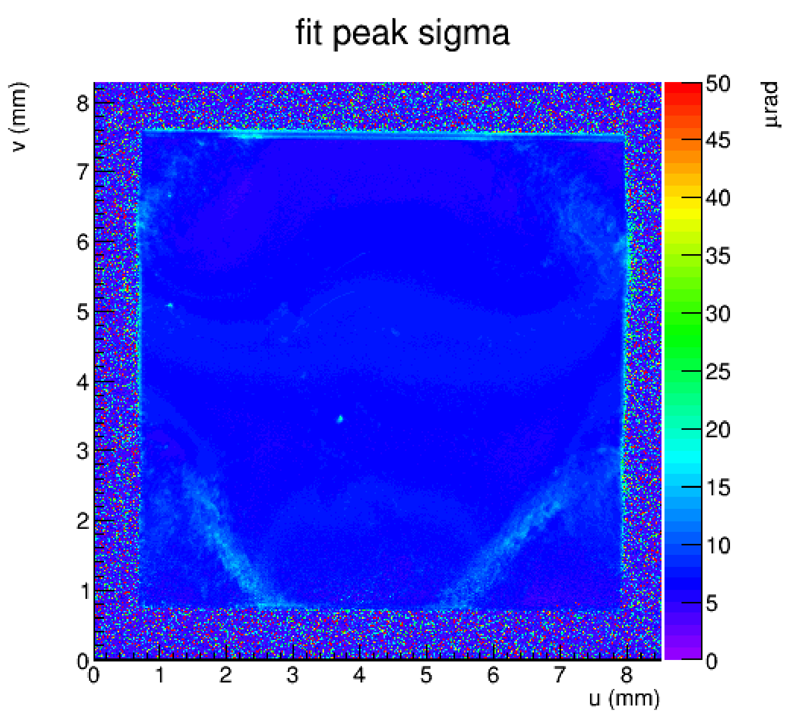

Figure: Rocking curve topograph of sigma for scan 14

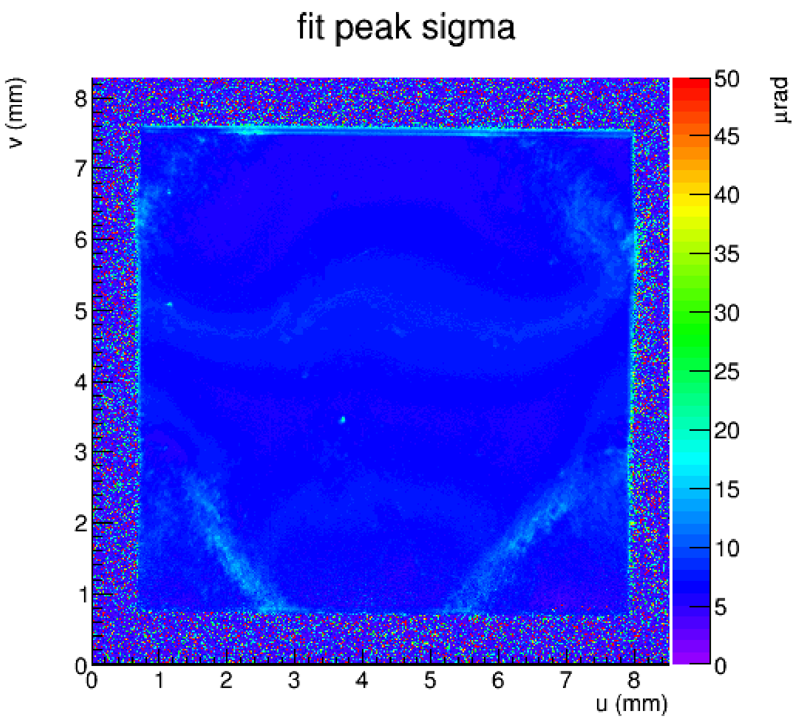

Figure: Rocking curve topograph of sigma for scan 15

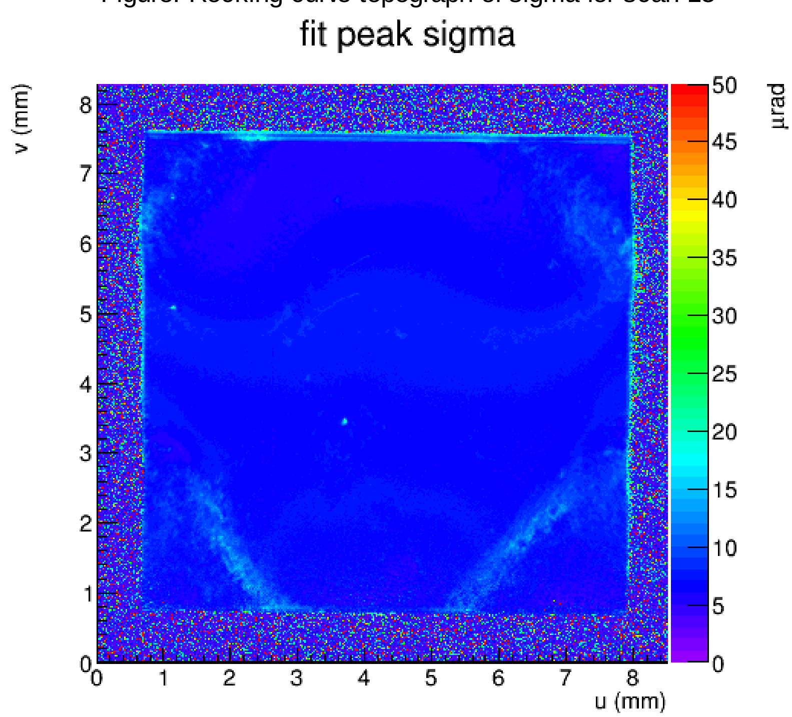

Figure: Rocking curve topograph of sigma for scan 16

And that’s a wrap.